Zeitschrift: IABSE reports = Rapports AIPC = IVBH Berichte
Band: 54 (1987)

Rubrik: Session 6: Cyclic and dynamic loading (applications)

SESSION 6

August 28, 1987 (afternoon)

Cyclic and Dynamic Loading (Applications)

Chargement cyclique et dynamique (applications)

Zyklische und dynamische Belastung (Anwendungen)

Chairman: A.C. Scordelis, USA

Invited Lecturers: J. Isenberg, W. Millavec, USA
Analysis of Reinforced Concrete Structures in Design Applications

H. Okamura, K. Maekawa, J. Izumo, Japan
Reinforced Concrete Plate Element Subjected to Cyclic Loading

Leere Seite
Blank page
Page vide

Analysis of Reinforced Concrete Structures in Design Applications

Analyse de structures en béton armé et application dans des projets

Betrachtungen von Stahlbetontragwerken beim Entwurfsprozess

Jeremy ISENBERG
Principal
Weidlinger Associates
Palo Alto, CA, U.S.A.

Jeremy Isenberg received BS and PhD degrees from Stanford and Cambridge Universities, respectively. A consulting engineer, he has worked in numerical methods applied to soil/structure interaction and reinforced concrete under earthquake and blast loading.

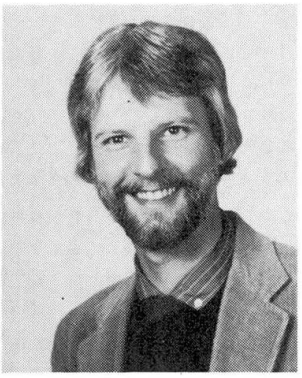

William Millavec received his BS and MS degrees in civil engineering from Case Western Reserve University. He has applied numerical methods to investigate and evaluate the survivability of soil/structure systems subjected to blast loading.

William MILLAVEC
Senior Res. Eng.
Weidlinger Associates
Palo Alto, CA, U.S.A.

SUMMARY

Design of complicated reinforced concrete structures can be effectively supported by finite element analysis using 32 bit minicomputers with multiple interactive terminals and batch communication to mainframe computers and graphics terminals. Multi-surface, cap-type constitutive models are used in an explicit, time-marching finite element computer program whose application in a design support example is illustrated.

RÉSUMÉ

Le projet de structures en béton armé compliquées peut être étudié au moyen d'analyses par éléments finis sur des mini-ordinateurs avec des terminaux multiples interactifs et en communication 'batch' avec de grands ordinateurs et des terminaux graphiques. Des modèles constitutifs multi-surfaces et 'cap-type' peuvent être utilisés dans un programme d'ordinateur avec des éléments finis. Un exemple d'application est donné.

ZUSAMMENFASSUNG

Entwurf und Berechnung komplizierter Stahlbetonkonstruktionen können hilfreich unterstützt werden, wenn man von Finite-Elemente-Programmen auf einem 32-bit-Minicomputer mit mehrfachen interaktiven Arbeitsstationen und Zugriff auf einen Zentralrechner und graphische Stationen Gebrauch macht. Materialgesetze mit mehrfachen, nach aussen offenen, Bruchgrenzflächen werden in einem expliziten, zeitgesteuerten Finite-Elemente-Programm benutzt, deren Anwendung in einem Beispiel gezeigt wird.

1. INTRODUCTION

Dynamic, nonlinear analysis has only recently gained a role in design of reinforced concrete structures to resist earthquake and explosive loads. This is due to modeling complexity and computer costs and to the perception that the results are too cumbersome to be integrated in a design process. This paper illustrates how recent advances in computer and graphics hardware encourage the use of advanced methods in design by making it easy to display snapshots of field quantities such as deformed shapes and distribution of moments and shear. These data show critical parameters for design and their locations. This is in contrast to the usual time history output which, even if it contains the peak response, does little to improve insight into overall response. This paper shows one approach having a beneficial effect on design due to exploiting hardware advances.

There are two approaches to generating and displaying response data in support of structural design. In the first, all computations are performed and postprocessed on a remote mainframe (CRAY or CDC CYBER, for example). User interaction is by telephone through a terminal connected to a modem. Graphical results are sent by mail or images are transmitted over the telephone to be displayed at the user's site. Often, the low data transfer rate associated with this approach impedes the analysis process so that it becomes impractical to vary design parameters quickly.

The alternate approach is to maximize analytic work done locally. The largest calculations are still performed at a remote site. However, once computed, the response data are transferred to the in-house computer system using an efficient file transfer protocal (such as HASP). Once local, the response data can be postprocessed and graphically displayed in many different ways without being constrained by telephone transfer rate limitations.

There are two main alternatives in acquiring in-house computer hardware (see Fig. 1). They are a multi-user minicomputer system or a single user workstation system. The minicomputer system is the least expensive approach to support a number of users who routinely create and share data files, perform analyses and postprocess results. Software and peripherals, such as graphics terminals, must be integrated by the user. Typical minicomputer systems which can support this type of work are the VAX and PRIME 32-bit processor machines.

Workstations provide a powerful computing environment dedicated to a single user. These machines are supermicrocomputers which provide integrated data entry, analysis and graphical display. Workstations produced by APOLLO and SUN are typical examples of engineering workstations. Most workstations run UNIX and support FORTRAN. In their simplest configuration, they typically have several megabytes of random access memory, about 60 megabytes of disk storage and special peripherals which support interactive modeling.

All are equipped with high quality graphics monitors having on the order of 1280 x 1024 resolution. A network of work-stations which allows file sharing between machines can be achieved using ETHERNET. File servers are also available for these networks.

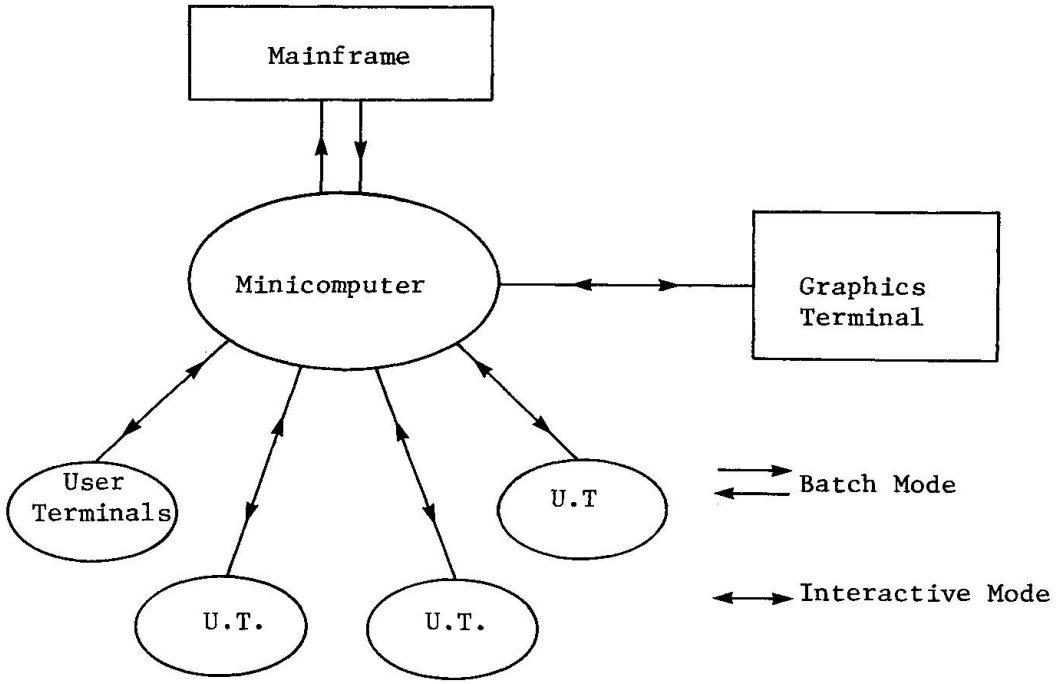

a. Multi-user minicomputer system

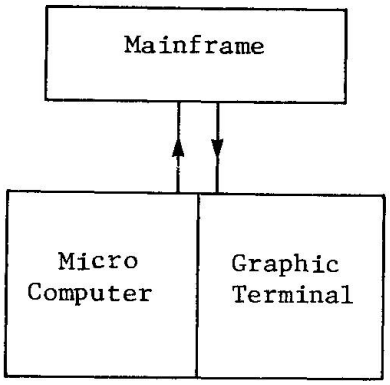

b. Single user workstation

Figure 1. Hardware alternatives which provide design support.

The choice of a minicomputer or workstation approach is dictated by the type of work, workload and number of users which the system is required to support. The workload during both daytime and nighttime hours should be considered in the selection. A workstation gives more power to a single user; the minicomputer distributes resources among a number of users. A minicomputer system is probably more expensive than a single workstation but is less expensive than a number of workstations.

Regardless of which hardware option is adopted, there is incentive to make modeling approximations that focus computer resources on the response of the reinforced concrete members. This is especially so in design support analyses where fast turnaround is needed to assess design alternatives. In analysis of explosive effects, there is often a protective layer of soil or other material which acts to mitigate the shock. It is essential to include the effect of this layer and desirable not to devote much resources to it. Methods for reducing the size of the soil domain in such problems are shown in Fig. 2. The first illustrates a reduced grid coupled with a suitable absorbing boundary. A series of models with progressively reduced soil cover is compared with a simulation standard. Excellent estimates of peak velocity response are obtained for the smallest grid, with a savings in processing time of a factor of order 50 relative to the baseline model. Greater economies are possible in 3-D problems. For flat-roof structures of the type considered in the example given below, there is little interaction between roof and sidewall; in such cases it is possible to reduce the model to a slab with overlying soil [Ref. 1].

The second method for reducing the size of a model is a decoupling approach in which the dynamic soil-structure interface stresses are computed from the following wavefront approximation.

$$\sigma_{int}(t) = \sigma_{ff}(t) + \rho c \, (v_{ff}(t) - v_{str}(t))$$

In this case, a preliminary free field analysis is performed to obtain the free field stress and partical velocity components normal to the structure. In highly nonlinear soils, the wave speed c is a function of stress level; a constant value assumed to be equal to the unloading wave speed is usually a satisfactory approximation. Descriptions of decoupling approaches for various applications are given in [Ref. 2, 3, and 4].

Candidate designs which have been evaluated by the procedures described above include shallow buried boxes, cylinders and arches.

Assessment of candidate designs requires data on spatial variation of stress resultants and deflections which can be displayed as snapshots at various times. Times of interest can be found by searching output files for peaks. Computed peak responses to shock loading often include numerical

overshoot. Post-processing by digital filtering is usually preferable to artificial damping. Reduction in time step is required if such overshoot significantly affect interpretation.

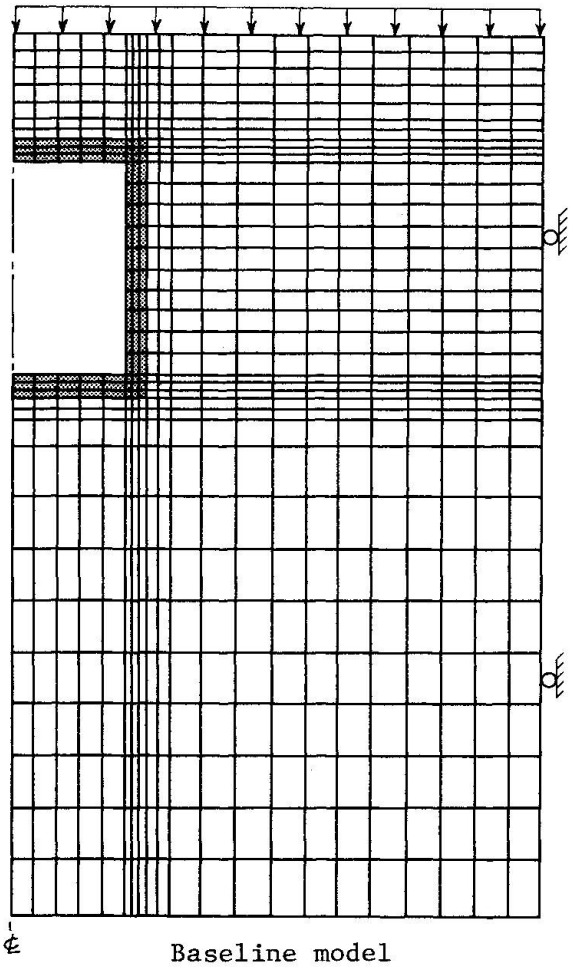

Baseline model

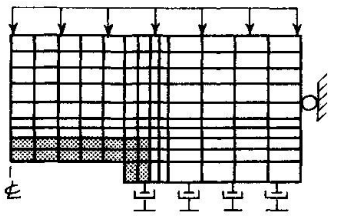

Reduced model with absorbing boundary

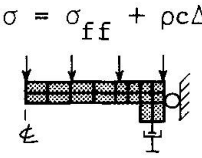

Reduced model with plane wave approximation for incident load

Figure 2. Finite element models for soil structure interaction and response of roof slab.

2. STRUCTURAL MODELING

2.1 Finite Element

The calculations presented below were performed using FLEX, a 3-D continuum finite element code developed at Weidlinger Associates [Ref. 5]. The standard eight-node isoparametric element, which employs a tri-linear interpolation function to represent the displacement field, is used to model the continuum. The hexahedron with one point quadrature to evaluate the element forces is a computationally efficient scheme for simulating wave propagation in a continuum. For rectangular grids, the approach is equivalent to the staggered grid method used in finite difference codes. The use of single point integration for the stresses results in zero stress deformation modes which, if not constrained, destroy

the solution [Ref. 6]. Control of hourglass instability has been proposed using a number of approaches. One scheme for stabilizing hourglass instability due to Flanagan and Belytschko [Ref. 7] has been implemented in FLEX. This approach isolates the hourglassing modes and provides them with an elastic stiffness to stabilize the mesh.

For dynamic calculations, the time integration algorithm in FLEX is an explicit method based on the central difference operator. This formulation is computationally more efficient than implicit methods for large nonlinear 3-D calculations, especially where small time steps are needed to resolve the steep gradients that occur at wavefronts. Efficiency is further enhanced by using a diagonal lumped mass matrix.

In a typical calculation, the elements vary in size and material type so that the time step required for numerical stability of the solution varies from element to element, (see Fig 3). A subcycling scheme has been implemented in FLEX to use time steps that are close to optimal in different regions. This method can significantly reduce the number of computer operations in the course of a solution. Each region is processed at a time step which is an integer multiple of the smallest time step in the model.

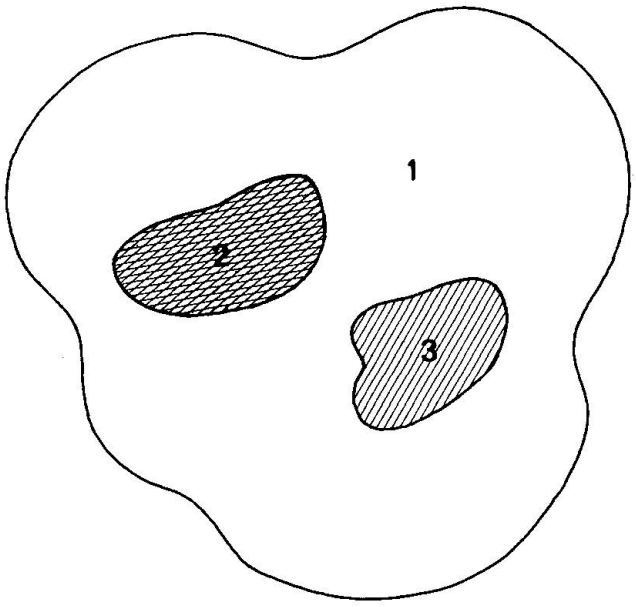

Typical subcycling ratios for buried reinforced concrete structure

Region	$\frac{h}{c}$ (time)	Δt (time)
1	10	8
2	5	4
3	1.5	1

h = element size
c = dilatational wavespeed

Figure 3. Subcycling approach uses integration time step (Δt) Appropriate to transit time ($h/_c$) in each region.

A static solution capability based on the conjugate gradient method has been incorporated into FLEX [Ref. 8]. This is an iterative method for solving the equations of equilibrium directly. Prior knowledge of the natural frequencies of the model required for solution by dynamic relaxation is not necessary.

The type of concrete model used predominantly in analysis of protective structures is based on the rate-independent, strain-hardening theory of plasticity. The example which is summarized here is the three-invariant cap model described in [Ref. 9, and 10]. The main features of the model include:

- An ideally plastic failure surface, a function of three stress invariants.
- An isotropically strain-hardening cap which introduces volumetric hysteresis and controls dilatancy (i.e., ratio of major to minor principal inelastic strains) for states of stress inside the failure surface.

The failure surface is in the form of a revised Willam and Warnke failure surface [Ref. 11], (Figs. 4 and 5). Its functional form in terms of stress invariants is given by:

$$f(\sigma_a, \tau_a, \theta) = \frac{\tau_a}{r(\sigma_a, \theta) f'_c} - 1 = 0$$

and

$$\sigma_a = \frac{1}{3}(\sigma_1 + \sigma_2 + \sigma_3) = J_1/3$$

$$\tau_a = \sqrt{(2/5)}\ \sqrt{J'_2} = \sqrt{2/5}\ \sqrt{(1/2) s_{ij} s_{ij}}$$

$$\cos 3\theta = (3/5)\ \sqrt{(6/5)}\ \frac{J_3}{\tau_a^3} = \frac{3\sqrt{3}}{2}\ \frac{J_3}{(\sqrt{J'_2})^3}$$

$$J_3 = (1/3) s_{ij}\ s_{jk}\ s_{k\ell}\ ;\ s_{ij} = \sigma_{ij} - \sigma_a$$

where J_1 is the first invariant of the stresses and hence is the mean pressure; τ_a is related to $\sqrt{J2}$, the second invariant of the deviatoric stresses; and θ is the Lode angle related to the third invariant of the deviatoric stresses J_3 and also τ_a.

Here $r(\sigma, \theta)$ represents the cross-sectional shape in the deviatoric plane and is given by

$$r(\sigma_a,\theta) = \frac{2r_2(r_2^2-r_1^2)\cos\theta + r_2(2r_1-r_2)\sqrt{4(r_2^2-r_1^2)\cos^2\theta+5r_1^2-4r_1r_2}}{4(r_2^2-r_1^2)\cos^2\theta + (r_2-2r_1)^2}$$

The functional forms for r_1 and r_2 used for the model are:

$$r_1(\sigma_a) = a_0 - a_1 e^{a_2(\sigma_a/f_c')}$$

$$r_2(\sigma_a) = b_0 - b_1 e^{b_2(\sigma_a/f_c')}$$

The functional form of the cap that intercepts the revised Willam and Warnke failure surface in a plane is

$$f_c = \frac{R^2-\delta^2}{r^2(L-\delta,\theta)f_c'^2}\frac{\tau_a^2}{f_c'^2} + \frac{(\sigma_a-L)^2}{f_c'^2} - \frac{(X-L)^2}{f_c'^2} = 0$$

where

$$X(\varepsilon_v^p) - L(\varepsilon_v^p) = -R(\varepsilon_v^p)$$

$$\delta = \delta(\varepsilon_v^p) \quad ; \quad R = R(\varepsilon_v^p)$$

and two forms of hardening rule for the cap have been explored, as follows:

$$\varepsilon_v^p = W\left[e^{\bar{D}(X-X_0)} - 1\right] \qquad X = X_0 + C_1\varepsilon_v^p + C_2 \ell n \cosh(-C_3\varepsilon_v^p)$$

$$+ C_4 \ell n \cosh(-C_5\,\varepsilon_v^p)$$

The quantities X, L and R, defined in Figs. 3 and 4, represent the intercept on the hydrostatic axis and maximum value of σ_a for the semi-major axis of the elliptical variation of the cap cross section with regard to σ. X_0 defines the initial position of the cap. The quantities W and D (or C_1 through C_5) define the hydrostatic hardening and are fit to hydrostatic stress-strain curves. The constitutive laws invoke the conventional flow rules of plasticity theory and the yield and loading criterion.

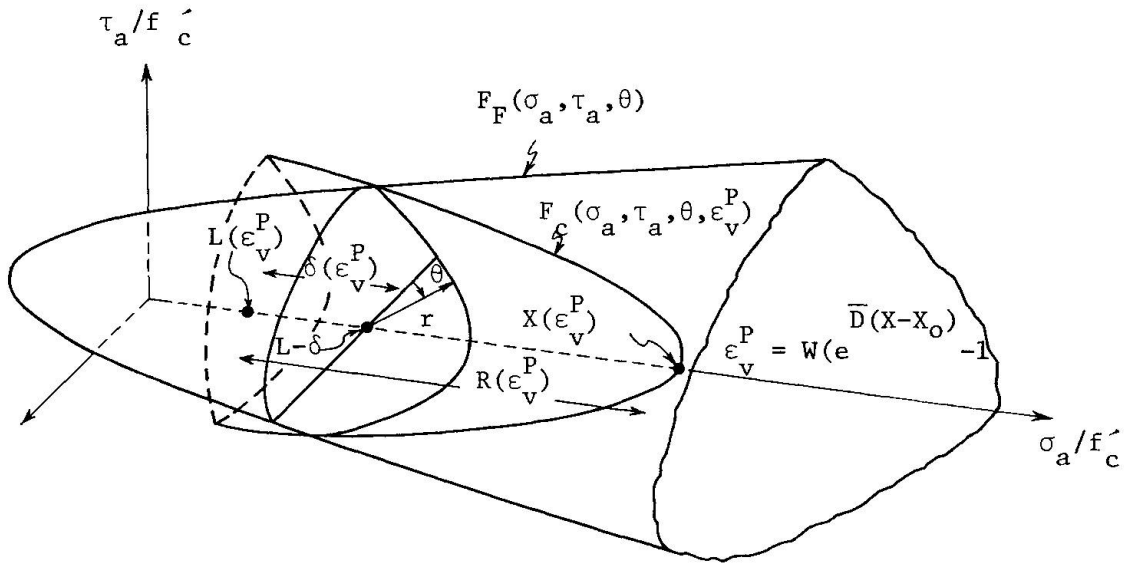

Figure 4. Configuration of cap in relation to failure surface.

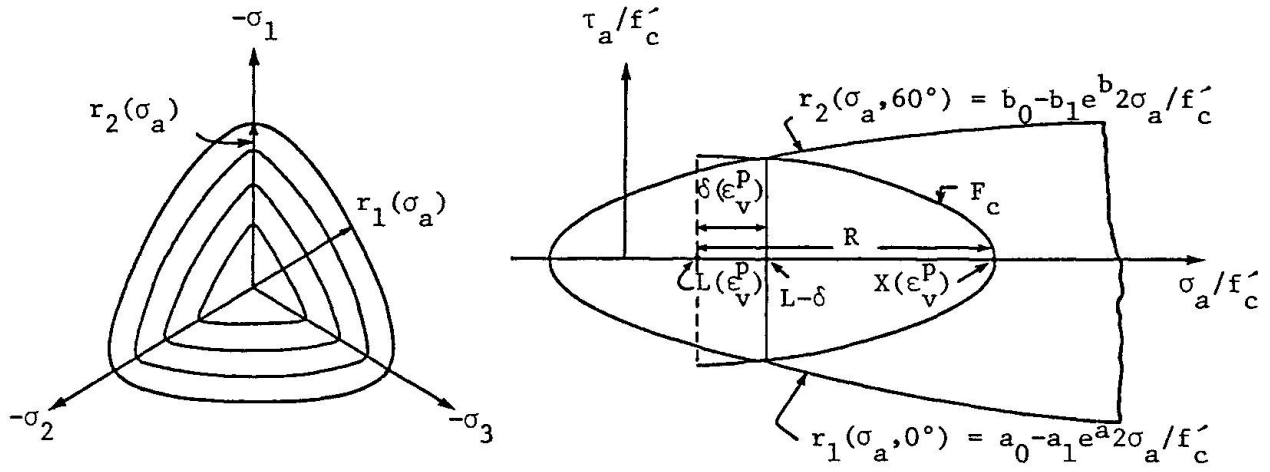

a. Deviatoric section b. Hydrostatic section

Figure 5. Cross section of cap and failure surface.

The enhancement of concrete strength due to strain rate effects in a rate-independent model requires the analyst to estimate the anticipated strain rate induced by the primary loading in the calculation. An enhancement factor is obtained from laboratory tests performed at a comparable strain rate. The initial concrete strength in the calculation is then adjusted by the enhancement factor. Modifications, similar to the viscoplastic model of Perzyna [Ref. 12] are being implemented to eliminate the ad hoc procedure approach, the rate of plastic straining is assumed to be proportional to the difference between a stress function and a quasi-static yield limit. This leads to stress relaxation from a dynamically induced peak back to the quasi-static

yield surface at a rate that depends on the strain rate.

The behavior of plain concrete is typically brittle at low confining pressures and becomes increasingly ductile with increasing confinement. The ductility inherent to plastic and viscoplastic material models is an appropriate approximation at high confining stresses, but at low confinement tends to overpredict the residual strength. The development of a rate-dependent, damage accumulation model is currently underway to address strain softening of plain concrete. The model is based on the concept of irreversible, isotropic damage. As a material is loaded into the softening range, spherical voids are assumed to form. Damage is defined as the ratio of these voids to the original volume. Damage is assumed to accumulate whenever the effective stress lies on or above the yield surface; that is, damage accumulation coincides with volumetric dilation. In spite of the simplifying assumptions required, this model is viewed as a significant improvement over unlimited ductility.

Modeling of the reinforcing bars is accomplished by the use of an explicit rebar element. Figure 6 shows a typical reinforcing detail for a structure and the modeling approximation. The strain in each bar is assumed to be equal to the strain in the continuum element evaluated at the centroid, and in the direction of the bar axis. The bar is assumed to be elastic, ideally plastic; the stress is uniquely a function of axial strain and stress history. Ideal bond conditions are assumed between the plain concrete and reinforcing bars. The primary goal of modeling reinforcing in this manner is to represent the confining effect of steel bars on plain concrete.

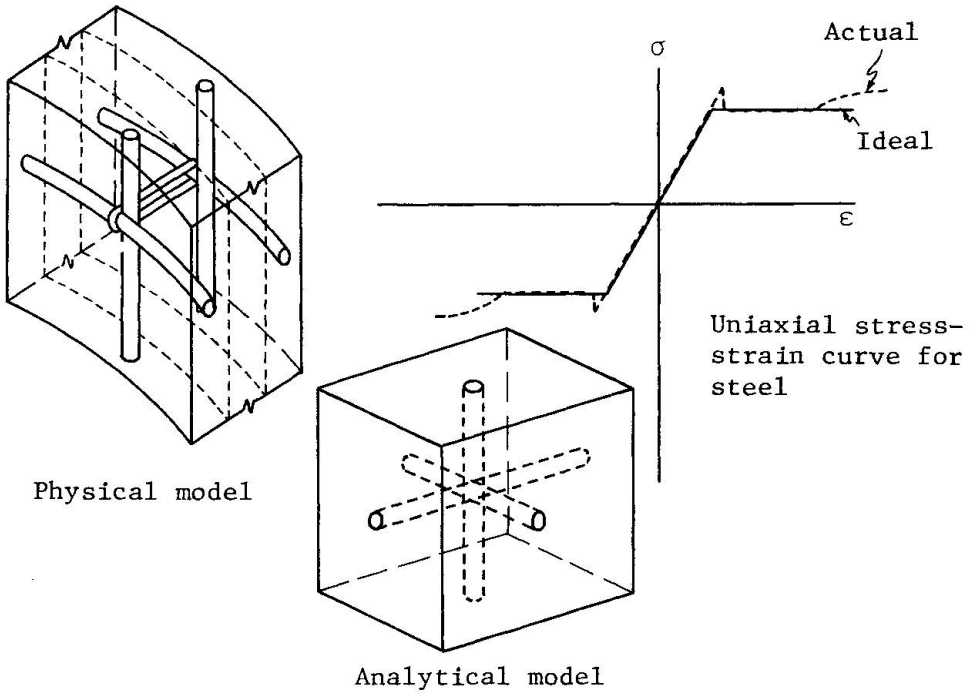

Figure 6.

This model accurately predicts the response of designs that survive explosive effects with light to moderate damage. Predictions of failure require interpretation based on extensive previous correlation with field test data.

3. EXAMPLE

Calculations supporting the design of a complex structure rarely consider the entire configuration. Typically, the design is decomposed into an assembly of components which are analyzed individually. The detail to which these structural elements are modeled depend on requirements to characterize the role of the element in the physical structure as well as the number of design parameters to be considered. Figure 7 describes the evolution of a computational model from the complete configuration to a bare roof slab subjected to a loading obtained from a simplified soil/structure interaction algorithm. In this case, the design of the roof slab has been completed, and a 3-D finite element model was constructed to perform validation calculations for two threat scenarios. The threats consisted of detonations on the burster slab above centerspan ($x = 0$, $y = 0$), (Case 1), and above the center of the short span near the long span support ($x = 0$, $y = 10\ell_y/11$), (Case 2). The initial conditions for the dynamic analyses were obtained from a static calculation of the slab loaded by the weight of the burster slab and overburden material. The decoupling scheme, described in section 1, was employed to evaluate the soil/structure loading. The energy coupling of the detonation into the ground and ground shock approximations used for the free-field definition were obtained from Ref. 13. The inherent symmetry of the roof slab and the location of the bursts permitted reduction of the required model to one-quarter of the roof slab. The discretization of the slab consisted of five-single-integration point elements through the thickness, and an overall element aspect ratio of one; resulting in a total of 12,615 elements. In an effort to obtain an accurate representation of the bending restraint at the wall without modeling the wall, the portion of the roof over the wall was included in the model. A horizontal roller support condition was then applied to the bearing surface, which eliminates wall rotations and displacement. An additional constraint, in which each row of nodes along exterior vertical edge of the slab were permitted to translate rigidly with no rotation, was imposed. This boundary condition prevents an unrealistic build-up of in-plane thrusts which artificially enhance the moment and shear capabilities of the slab, that full in-plane and rotational fixity would produce. The plain concrete is modeled using the rate independent, strain hardening version of the concrete model. The reinforcing bars are modeled explicitly using the rebar elements. The simulation output consists of a minimal number of velocity histories used primarily for diagnostic purposes, and a large number of displacement and resultant force snapshots, used for field display useful to

the designer. The model requires approximately one million words of central memory and 6 cp-minutes per 10 ms of structural response on a CRAY-1 computer. Peak response occurs at about 20 ms for the cases presented here.

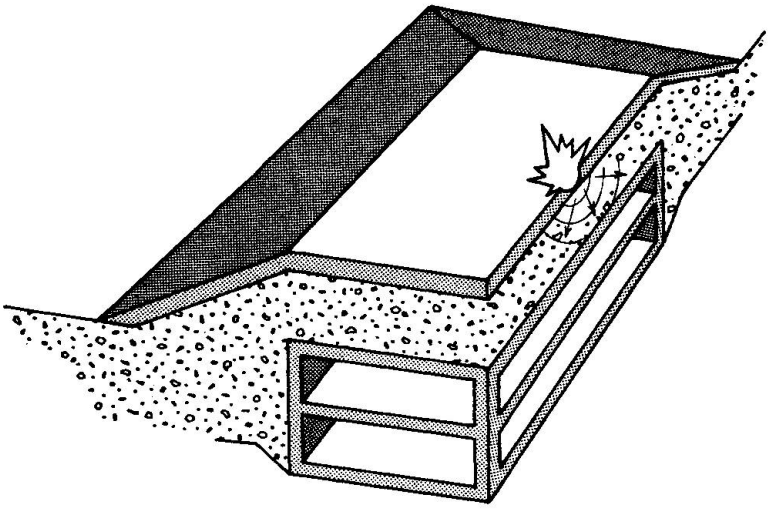

a. One-quarter of the structure.

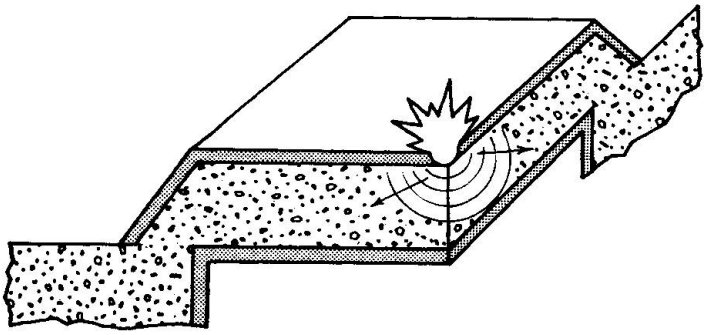

b. Roof slab including burster slab and overbursts

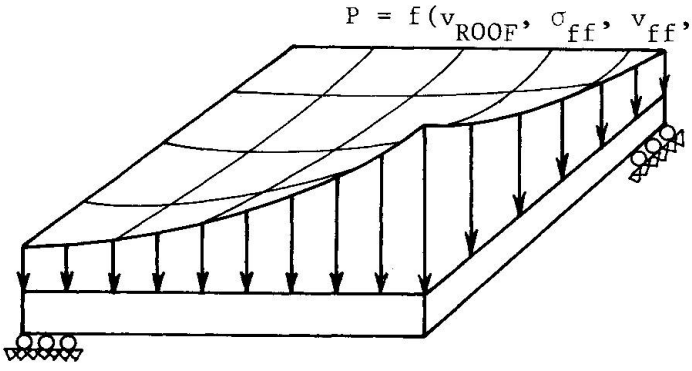

c. Roof slab model and semi-empirical interaction model

Figure 7.

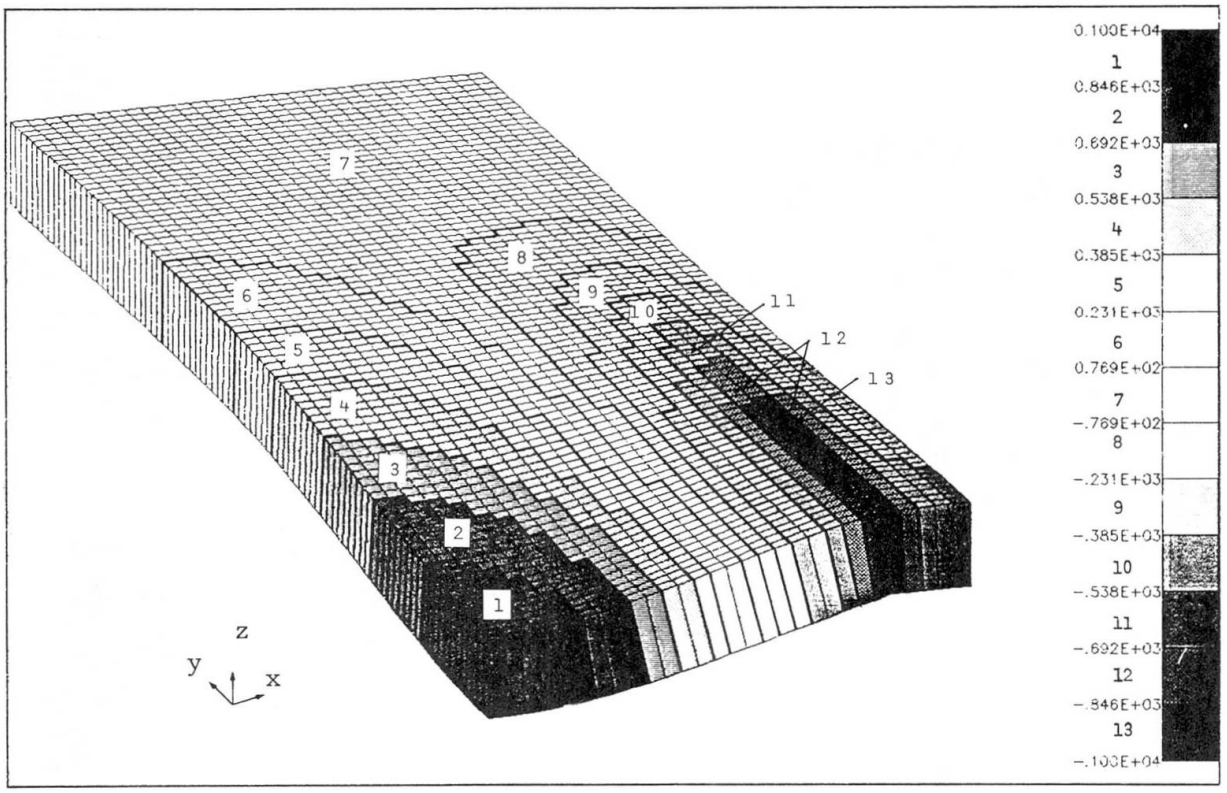

Short span moments (M_{yy}) for Case 1 at 20 ms.

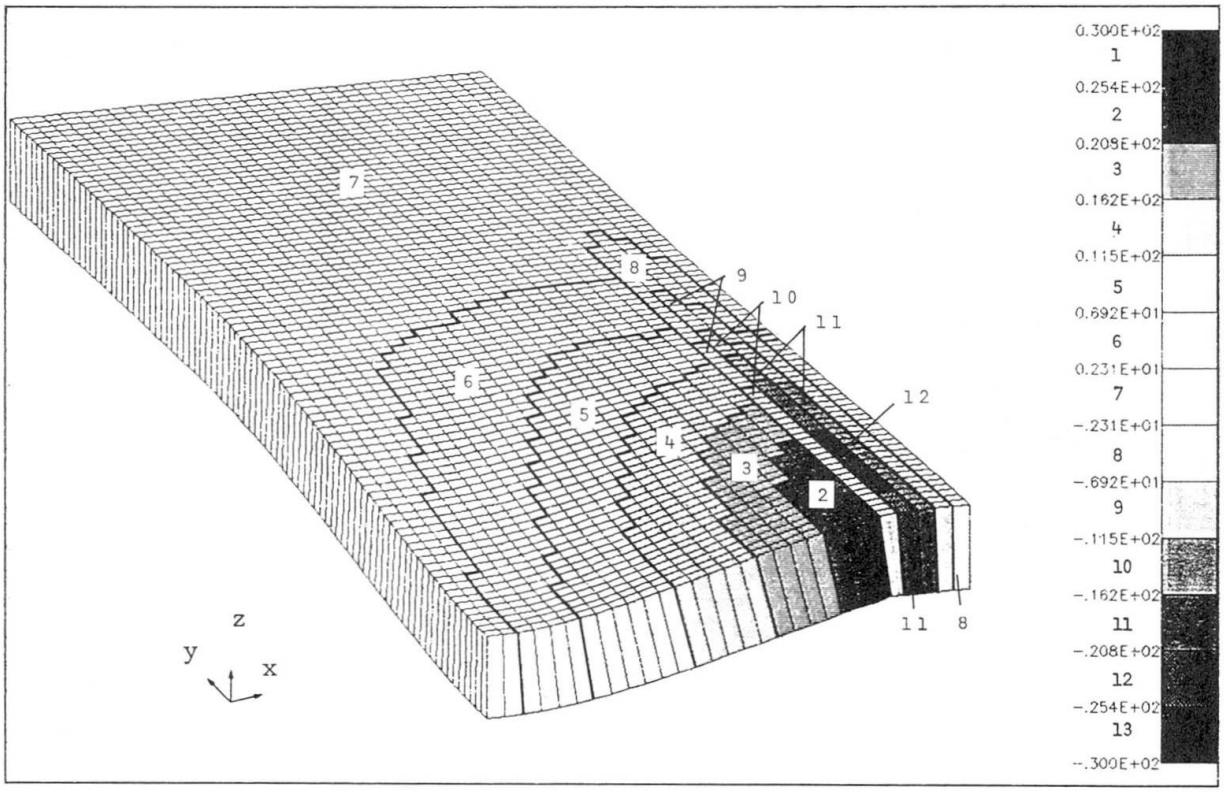

Short span shear (V_{xz}) for Case 1 at 20 ms.

Figure 8.

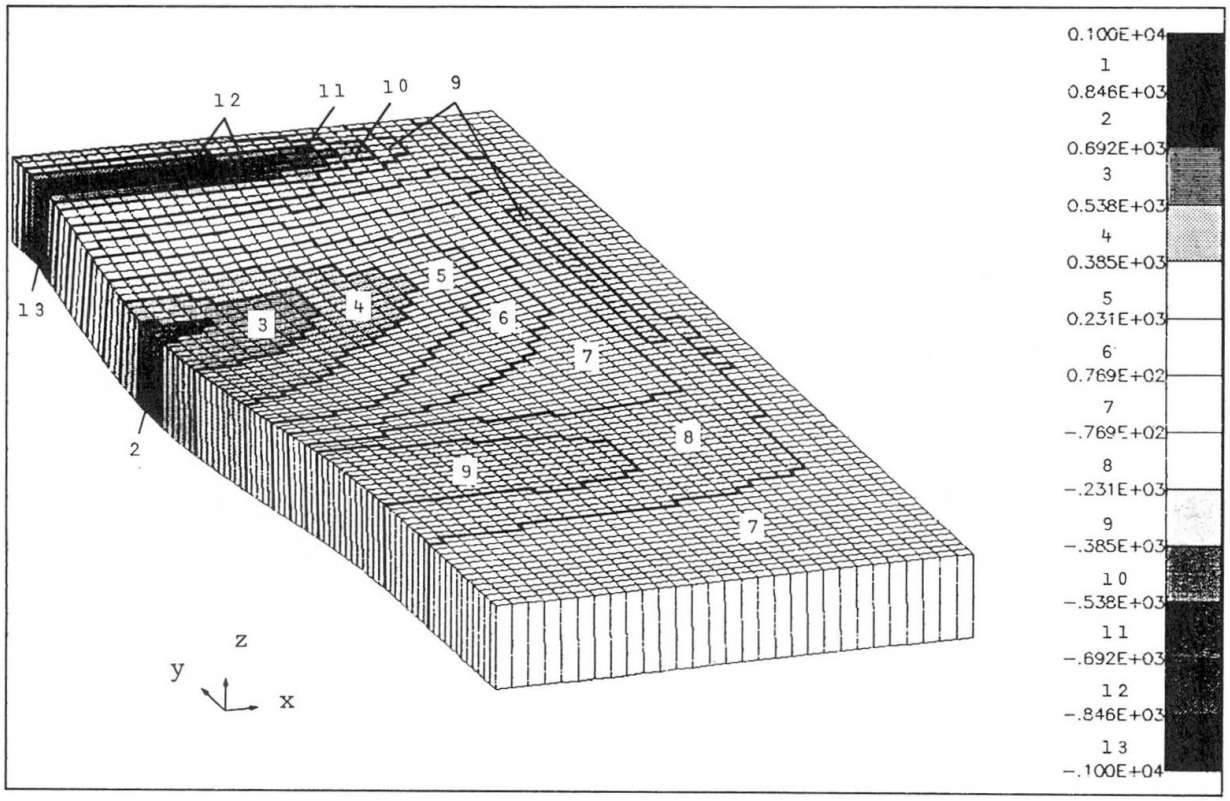

Long span moments (M_{xx}) for Case 2 at 20 ms.

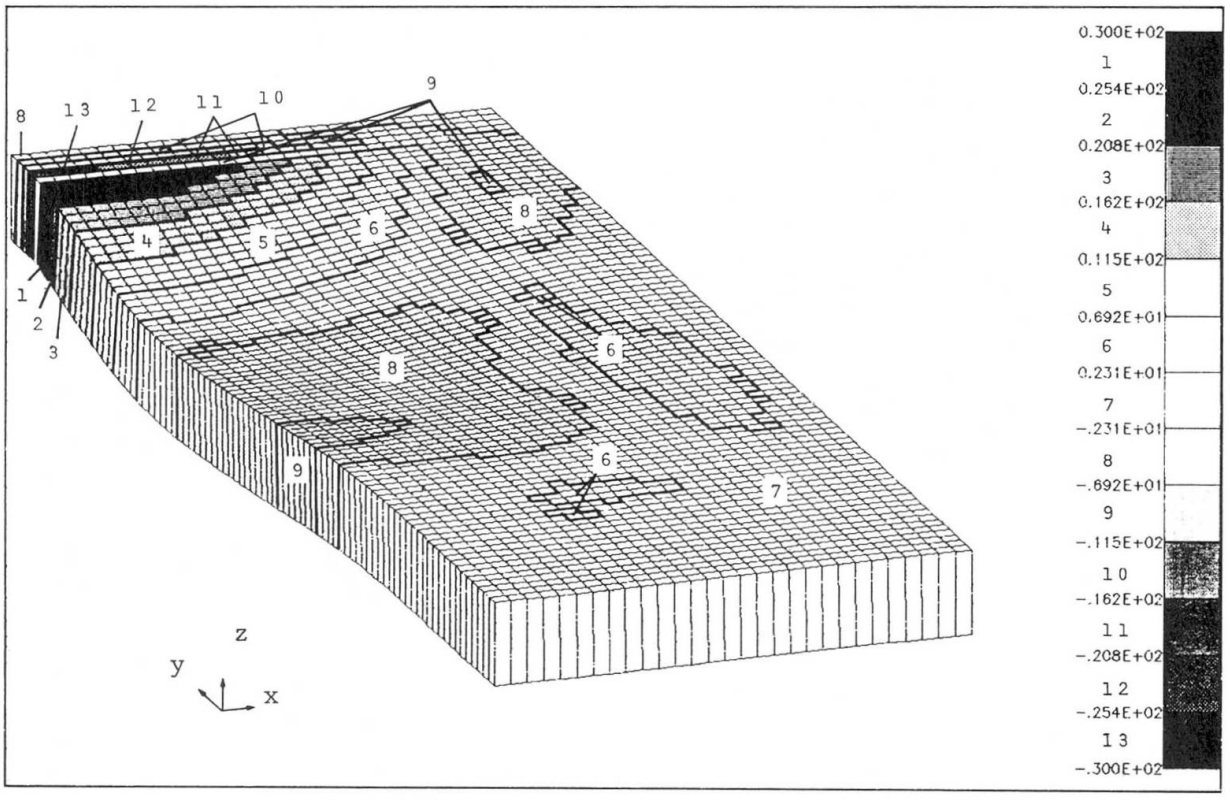

Long span shear (V_{yz}) for Case 2 at 20 ms.

Figure 9.

Figure 8 shows the short span bending moments and shear forces in the slab near peak response for Case 1. The rapid decay of these quantities in the long direction indicates one-way response of the roof. The superposition of the bending moments and shears on the deformed mesh provide the designer with a near complete picture of the structural response. The advantages of viewing a few of these snapshots at discrete times over examining a large number of history plots is readily apparent. The short span response for Case 2 is comparable in magnitude to Case 1 with the peaks occurring directly below the burst. Figure 9, which shows the bending moment and shear in the long direction, indicates the degree of two-way action occurring for this case. A locus of critical sections for the roof slab can be deduced by combining the results of these attacked scenarios.

4. SUMMARY

This paper discusses how nonlinear dynamic finite element analysis capabilities for reinforced concrete structures can be accessible to a design office. The hardware alternatives considered ranged from total dependence on a remote mainframe to a configuration which employs a complement of small local as well as remote computers. The local system is used for pre- and postprocessing, while the analysis itself is performed remotely. The local systems discussed included mini-computers suitable for supporting a large number of users and work stations for single users which could be networked to accommodate a multi-user environment. All configurations considered include a high resolution color graphics terminal. The feature enables the analyst to view color-coded snapshots of field quantities, such as stress, strain, forces, and moments, superimposed on deformed meshes. This provides a powerful tool to the designer who can readily indentify the magnitude and location of critical response quantities.

Given this hardware environment, detailed design support calculations can be performed and easily interpreted. A continuum code, FLEX, which is particularly suited to this class of problems is presented. An eight-noded, single integration point hexahedron, which is explicitly integrated in time, provides the foundation of the code. The plain concrete is modeled using a three invariant version of the cap model. Model development efforts are currently directed towards including strain rate effects and strain softening. A rebar element for explicitly modeling the reinforcing bars, completes the features necessary for the modeling reinforced concrete structures.

The impact of these hardware and software advances are demonstrated in the analyses of a 3-D roof slab model subjected to a blast loading. The effectiveness of these improvements is evident in the ease of assessing the structural response from a few selected displays of field quantities.

REFERENCES

1. WONG, F. S. and WEIDLINGER, P., "Design of Underground Shelter Including Soil-Structure Interaction Effects", Proc of a Symposium on Interaction of Non Nuclear Munitions with Structures, U.S. Air Force Academy, May 10-13, 1983.

2. NELSON, I. and ISENBERG, J., "Soil Island Approach to Structure/Media Interaction", Numerical Methods in Geomechanics, CS Desai (Ed) Proc 2nd International Conference on Numerical Methods in Geomechanics, Virginia Polytechnic Institute and State University, June 1976, p41-57.

3. LYSMER, J. and KUHLEMEYER, R. L., "Finite Element Dynamic Model for Infinite Media", J. Eng. Mech. Div., Proc ASCE V95 No.EM4, August 1969, p859-877

4. SANDLER I, "A Method of Successive Approximations for Structure Interaction Problems", Computational Methods for Infinite Domain Media-Structure Interaction, AMD-Vol. 46, Presented at The Winter Meeting of ASME, November 1981.

5. VAUGHAN, D. K., "FLEX Users Manual", Weidlinger Associates WA-MP-UG 8298 December 1982, Revised March 1985

6. IRONS, B. and AHMAD, S., "Techniques of Finite Elements", Ellis Horwood, Chichester, England, 1980.

7. FLANAGAN, D. P and BELYTSCHKO, T., "A Uniform Strain Hexahedron and Quadrilateral with Orthogonal Hourglass Control", International Journal for Numerical Methods in Engineering, Vol. 17, p679-706, 1981.

8. PILAND, T. J., ISENBERG, J. and GHABOUSSI, J., "Finite Element Analysis of Misty Rain Tunnel Intersection", Weidlinger Associates DNA Report R8626, May 1986.

9. LEVINE, H. S., "A Two-Surface Plastic and Microcrocking Model for Plain Concrete", Nonlinear Numerical Analysis of Reinforced Concrete, Winter Annual Meeting ASME, Phoenix, AZ, November 14-19, 1982.

10. LEVINE, H. S. and MOULD, J. C., "A Three-Invariant Cap Model for Concrete Soil and Rock: Computational Aspects", ASME/ASCE Summer Mechanics Conference, Albuquerque, NM, June 1985.

11. WILLAM, K. J. and WARNKE, E. P., "Constitutive Model for the Triaxial Behavior of Concrete", IABSE Seminar on Concrete Structure Subjected to Triaxial Stresses, Paper III-1, Instituto Specimentali Modelli e Strutture, Bergamo, Italy, May 1974

12. PERZYNA, P., "The Constitutive Equations for Rate Sensitive Plastic Materials", Quarterly Appl. Math., Vol. 20, Nov. 4, 1963.

13. "Fundamentals of Protective Design for Conventional Weapons", Structures Laboratory, Department of Army, Waterways Experimental Station, Corps of Engineers, Vicksburg, Mississippi, July 1984

Reinforced Concrete Plate Element Subjected to Cyclic Loading

Elément de dalle en béton armé soumis à des charges cycliques

Stahlbetonplattentragwerken unter Wechsellast

Hajime OKAMURA
Professor
Univ. of Tokyo
Tokyo, Japan

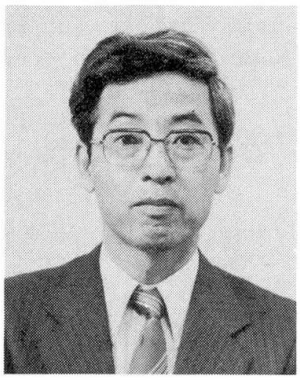

Kohichi MAEKAWA
Assoc. Professor
Univ. of Tokyo
Tokyo, Japan

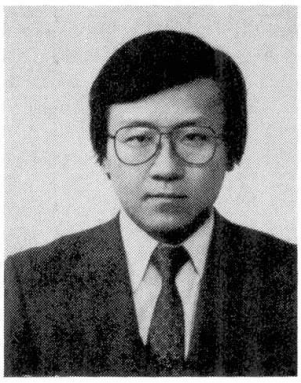

Junichi IZUMO
Assist. Lecturer
Univ. of Tokyo
Tokyo, Japan

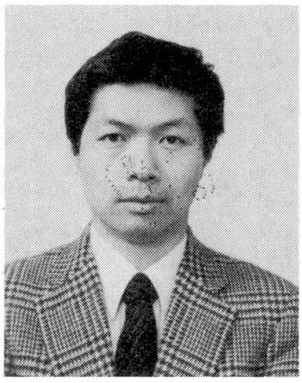

SUMMARY

A comprehensive model has been developed to analyze the behaviour under reversed cyclic loading of reinforced concrete plate elements, with the reinforcement uniformly distributed. The model comprises tension, compression and shear models of cracked concrete, and a model for reinforcement in the concrete; and also a so called smeared crack model is incorporated. The applicability of this model has been verified by comparing the predictions with published experimental results of reinforced concrete panels.

RÉSUMÉ

Un modèle global a été développé pour étudier les comportements d'éléments de dalles en béton armé, avec des barres d'armature distribuées uniformément, sous l'effet de charges cycliques alternées. Le modèle comprend des cas de tension, compression et cisaillement de béton fissuré, ainsi qu'un modèle de renforcement du béton; il est aussi envisagé un modèle de fissuration homogénéisée. La valeur de ce modèle a été vérifiée en comparant les prévisions avec les résultats expérimentaux publiés pour des panneaux en béton armé.

ZUSAMMENFASSUNG

Ein umfassendes Modell zur Analyse des Verhaltens von Betonflächentragwerken mit gleichmässig verteilter Bewehrung unter Wechselbelastung wurde entwickelt. Das gesamte Modell enthält Zug-, Druck- und Schubmodelle sowie ein Modell für Stahlbeton und behandelt auch verteilte Rissbildung (smeared crack). Die Anwendbarkeit des Modells wurde an Vergleichsrechnungen mit veröffentlichten Ergebnissen an Stahlbetonscheiben überprüft.

1. INTRODUCTION

The mechanical behaviors of reinforced concrete members under cyclic or reversed loading are being clarified by many experimental works. However, very few works have been done for analytical prediction of these behaviors [1] - [5], mainly because of the difficulty in modeling the cracked concrete appropriately. Due to the same reason none of the contestants was able to predict the behaviors for monotonic loading in the Collins' Competition [6]. Before predicting the behaviors of a reinforced concrete member, the behaviors of an element of that member should be predicted accurately.

For analysis of a plate element having distributed reinforcement, the smeared crack model is appropriate. We have been trying to develop material models [7] that are capable of acurately describing the behaviors of cracked concrete, and these models stood tests of comparison against experimental results on panels conducted by Vecchio and Collins or by Aoyagi and Yamada. The present model has been developed out of these models so as to include the cases of reversed cyclic loading.

2. MATERIAL MODELING

2.1 General

Reinforced concrete plate elements are often presented as a superimposition of concrete and reinforcement. In the concrete part, taking the y axis in the direction of cracks and the x axis normal to it, the constitutive laws of cracked concrete can be constructed with comparative ease in terms of tensile stiffness along the x axis and compression along the y axis as shown in Fig.1. The coordinates for the reinforcement is conveniently taken in the directions of the two reinforcement axes, and the constitutive equations for reinforced concrete can be obtained by superimposing the two elements by coordinate conversion. However, it is to be remembered that, because these rules are for the concrete and the reinforcement as element of a reinforced concrete, they can be different from those that are for isolated reinforcement or for isolated concrete.

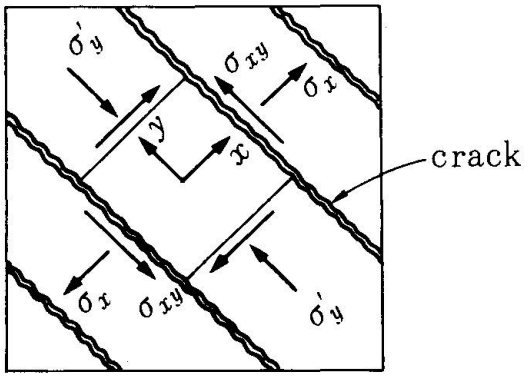

Fig.1 The coordinates for cracked concrete

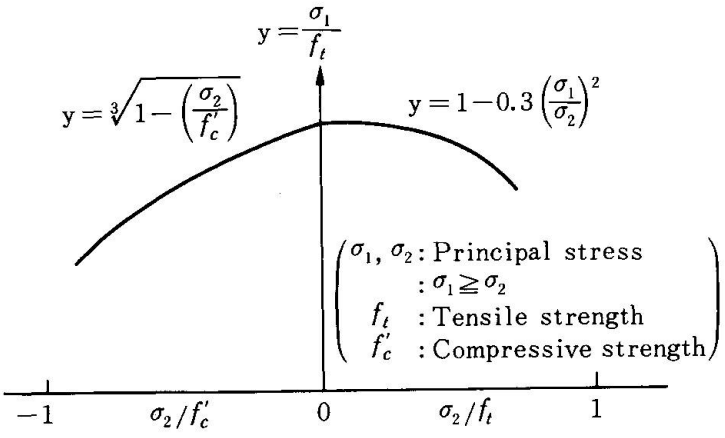

Fig.2 Cracking criteria of concrete under biaxial stress states [8] [9]

2.2 Cracking of Concrete

The cracking has been assumed to occur in the concrete when the principal tensile strain has reached the ultimate tensile strain. Here, the ultimate tensile strain is generally 0.01 to 0.03 %, but for the sake of simplicity, it was set to twice of the principal strain at the time when the stress acting on concrete has reached the tensile fracture envelope. This is to predict the occurrence of cracking with certain degree of accuracy even in the cases of nonuniform stress distribution.

As for the fracture envelope, those that have been proposed with emphasis on cracking under biaxial loading, one due to Niwa for compression-tension [8] and the other to Aoyagi and Yamada for tension-tension [9], have been adopted as shown in Fig.2. According to Maekawa, the fracture envelopes for monotonic loading are hardly affected by the loading path [10]. Another assumption has been that the concrete remains perfectly elastic until cracking as shown in Fig.3.

2.3 Tension Stiffening Model

Onset of cracking in reinforced concrete means that the concrete has lost its load carrying capacity at the plane of crack, and there the entire tensile force is borne by the reinforcement. In the portion between two cracks, however, concrete still bears up a part of the tensile force owing to the bond stress that transfers the tensile force from reinforcement to concrete. Therefore, reinforced concrete develops, even after it has been cracked, a higher stiffness than that of an isolated reinforcement. This increase of stiffness owing to concrete is generally known as the tension stiffening.

In order to accomodate this phenomenon, various proposals, such as a method that assumes either bond slip relation [11] - [12] or bond stress distribution [13], one that assumes maximum strain average strain relation for reinforcement [14] - [15], one that assumes directly the stress strain relation for reinfroced concrete [16] - [17], and one that assumes average stress average strain relation for concrete [18] - [19], have been advanced. Judging the method that presupposes an average stress average strain relation for concrete to be most convenient to apply to the plate elements, we have selected the one that is shown in Fig.4 [7]. The parameter c that is included in this model is to represent the bond, and a value of 0.4 is appropriate for ordinary deformed bars, while 0.2 fits well to the cases of welded mesh that Vecchio and Collins employed.

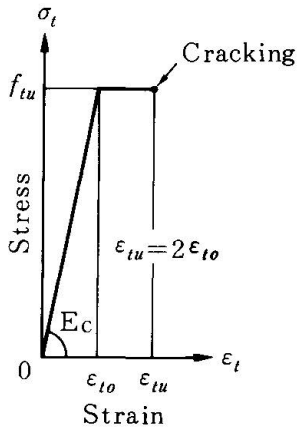

Fig.3 Stress strain relation of concrete for tension

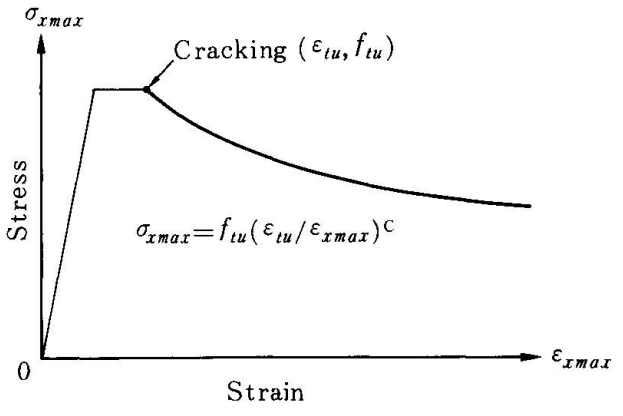

Fig.4 Tension stiffening model [7]

Values according to this model are compared with proposals by Morita and Kaku [20], and Vecchio and Collins [21] as shown in Fig.5.

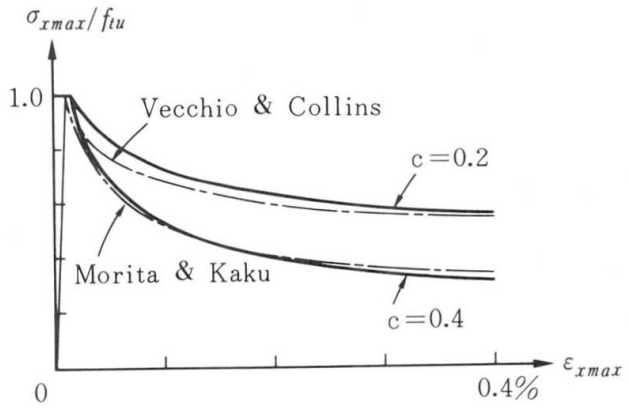

Fig.5 Tension stiffening model compared with the proposals by Morita and Kaku [20] and Vecchio and Collins [21].

The tension stiffening model on unloading and reloading has been developed on the basis of the experimental results of Tamai and Shima [22]. In the model, the stress acting on concrete was assumed to consist in the stress transferred from reinforcement by bond and that transferred by contact of crack surface and these two were individually modeled. The stress arising from bond was presented by a quadratic curve connecting the envelope and the origin for unloading, and by a straight line extending to the envelope for reloading as shown in Fig.6 and 7. As the contact of crack surfaces takes place the faster the larger the shear displacement along the crack, the tensile strain at onset of contact was taken to be a function of the shear strain. Unloading after contact was made to proceed elastically at a slackened stiffness, whereas the contact stress was made to become zero on reloading as shown in Figs.6 and 7.

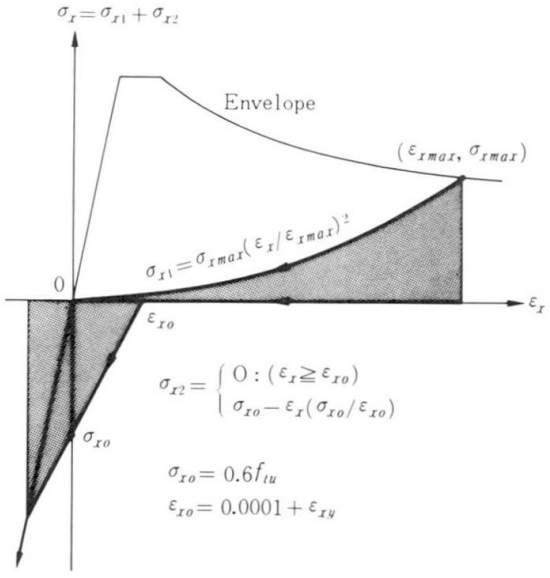

Fig.6 Tension stiffening model for unloading [22]

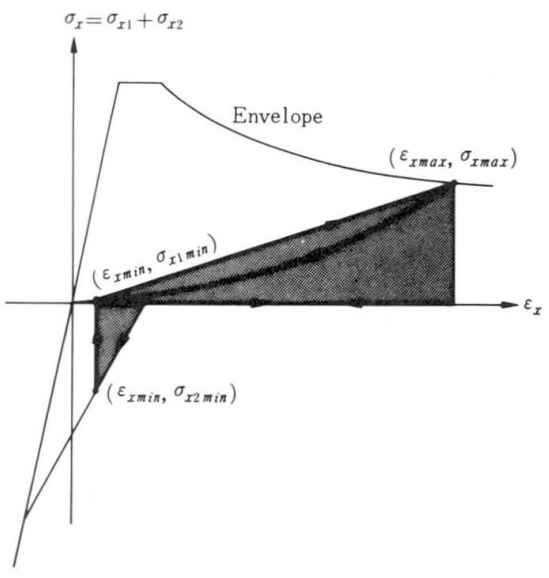

Fig.7 Tension stiffening model for reloading [22]

2.4 Compression Model of Cracked Concrete

For the compressive stiffness of concrete in the crack direction (y direction), modified Maekawa's model was used. In the Maekawa model[10], the initial elastic modulus Eo, the fracture parameter Ko, and the compressive plastic strain are introduced to define the envelope for compressive stresses and compressive strains, so that unloading and reloading can be conveniently described as shown in Fig.8. Since neither the fracture parameter nor the plastic strain changes inside the envelope, the internal curves are represented by straight lines of slopes EoKo, meaning that no energy is dissipated in the unloading and reloading. Although this is untrue, this assumption may well be tolerated for its merit of highly simplifying the calculation, provided that the energy consumed in compressive deformation of concrete is sufficiently small compared with the total expenditure of energy. Actually, modeling of increasing internal damages under cyclic loading is necessary to reasonably describe the energy consumption in the unloading and reloading process. For this purpose, a model has been completed recently by the present authors, which will be reported in due time.

The compressive plastic strain has been formulated, as shown in Fig.9, in terms of a single value function of the maximum compressive strain that the body had sustained in the past the strain right on the envelope. Furthermore, this formula has been experimentally demonstrated to be applicable even to the cases where cracks are present in parallel to the direction of compression [23].

The fracture parameter Ko, which is to represent the extent of the internal damage of concrete, has also been assumed to be a function of the maximum compressive strain as in the case of plastic strain as shown in Fig.10. However, the fracture parameter is affected by the cracks running in parallel to the comprssion direction. This is clarified by a compression testing of cracked reinforced concrete cylinders as shown in Fig.11 [23].

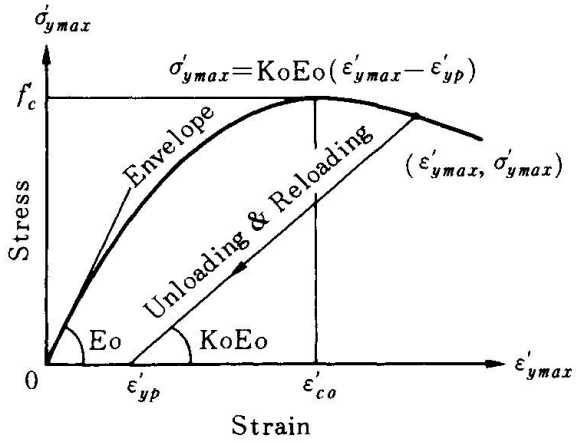

Fig.8 Maekawa model for compression [10]

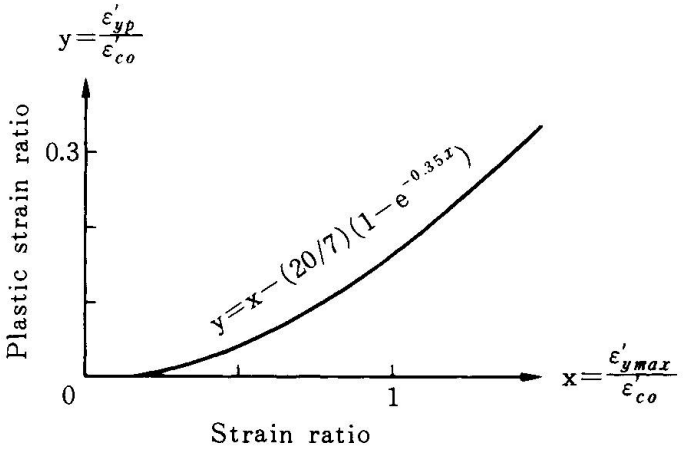

Fig.9 Plastic strain in terms of a function of the maximum compressive strain [10]

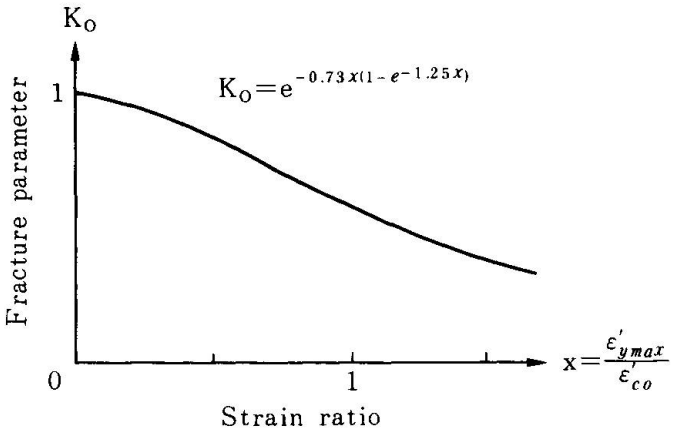

Fig.10 Fracture parameter for uncracked concrete [10]

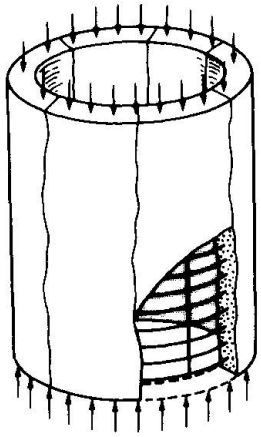

Fig.11 Compressive test specimens [23]

It has been pointed out by Vecchio and Collins that the apparent compressive strength and stiffness are decreased by cracks. Since these phenomena may be attributed mainly to stress relaxation taking place in the vicinity of cracks, we have elected to take a ratio of the fracture parameter K and that of uncracked concrete Ko as a function of the tensile strain in the direction normal to cracks. Namely, the parameter K was set to be the same as Ko for the tensile strain less than 0.12 %, be constant at 0.6 Ko for the tensile strain of over 0.44 %, and to change linearly in the intervening range as shown in Fig.12. For comparision, the strength ratios of the proposals of Vecchio and Collins [21], Cervenka [24], and Miyahara and Maekawa [23] are shown in the Fig.12.

The values obtained by the modified Maekawa model are compared with the experimental values due to Miyahara and Maekawa that include the cases of unloading and reloading with the tensile strain constant as an example. It will be seen in Fig.13 that agreement is quite satisfactory except for the lack of bulge in the unloading curve.

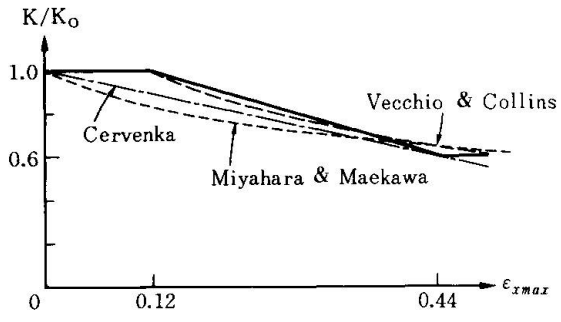

Fig.12 Relationship between the ratio (K/Ko) and tensile strain

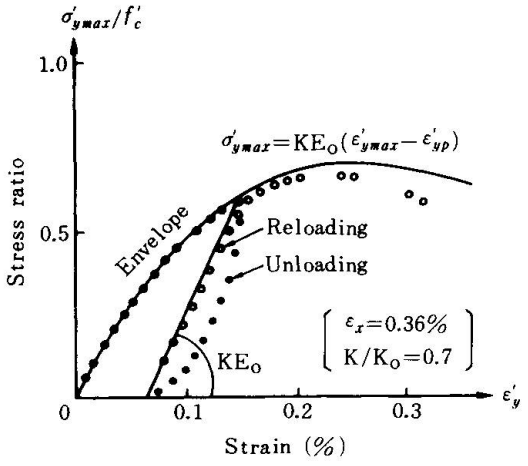

Fig.13 Modified Maekawa model versus experimental result [23]

To accomodate the plastic strain that is incurred in concrete when subjected to a compressive stress, the stress strain curve was shifted by that much amount of the compressive plastic strain toward the compressive stress as shown in Fig.14. Here, the tensile elastic modulus was assumed to be EoK, the same as for compressive stress, and the tensile strength to be Kft. These have been verified experimentally.

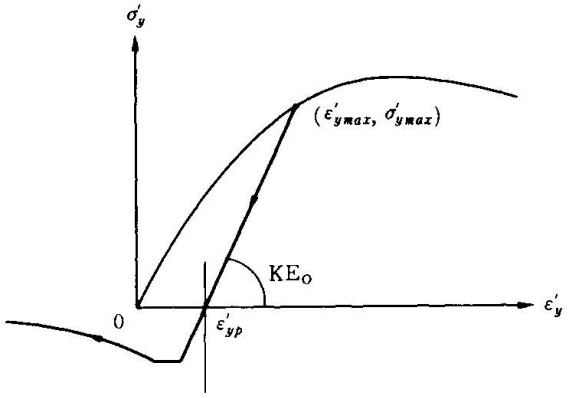

Fig.14 Constitutive laws of cracked concrete from compressive region to tensile region

2.5 Shear Transfer Model

Though many investigations have been done on the mechanism of shear transfer along cracks, the majority is concerned only with monotonic loading. We have developed a contact density model that applies well to cyclic loading, assuming each crack to consist of numerous contact planes oriented in various directions as illustrated in Fig.15. By giving appropriate distribution profiles to the orientations of the contact microsurfaces and to their effective areas, relation among the shear displacement, the crack opening and the shear stress has been formulated.

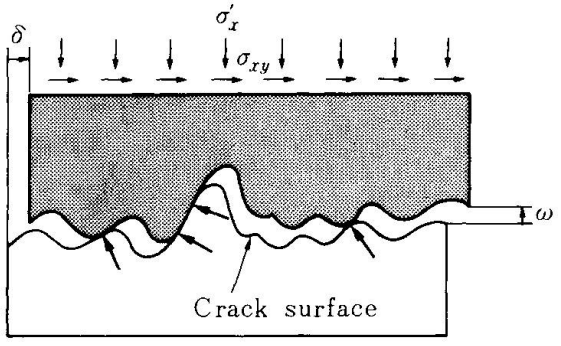

Fig.15 Shear transfer mechanism

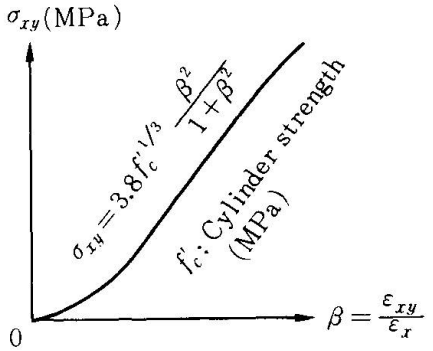

Fig.16 Shear transfer model

This model is described by an integral equation with regard to the directions of contact planes, and is able to predict the shear transfer behavior for any loading paths. When the loading is monotonic, in particular, this integral equation has an analytical solution, in which the shear stress is given by a uniquely determinable function of the ratio between shear displacement and the crack opening as shown in Fig.16. This function was considered to represent the envelope for the shear transferred stresses. Where, the ratio gives the orientation of a plane situated at a boundary between contacting surfaces and non contacting surfaces.

Though shear transferred stresses in the unloading and reloading can be calculated by this contact density model, it is not too well suited for analysis of reinforced concrete plate elements, because of the trouble of numerical intergration. When numerical integrations were actually conducted for many different paths, it was found that no great errors would be incurred even if the shear transferred stress were expressed uniquely by the ratio between the shear displacement and the crack opening. On the basis of this fact, it was decided that the shear transferred stress should move along a straight line that passed through the envelope point for the onset of unloading and the corresponding plastic point as shown in Fig.17.

Although this model is for a single crack, the average shear stiffnesses for elements containing multitude of cracks in a certain distribution can be presented by the average strain that is given by the relative displacement across a crack divided by the spacing to the next crack. In these cases, the ratio between the shear displacement and the crack opening coincides with that of shear strain and tensile strain, and the shear stress acting on an element containing cracks may be evaluated solely by the shear strain and the tensile strain regardless of the crack spacing. The compressive stresses arising from shear transfer and acting normal to the crack plane are presented in terms of these average strain ratio as shown in Fig.18.

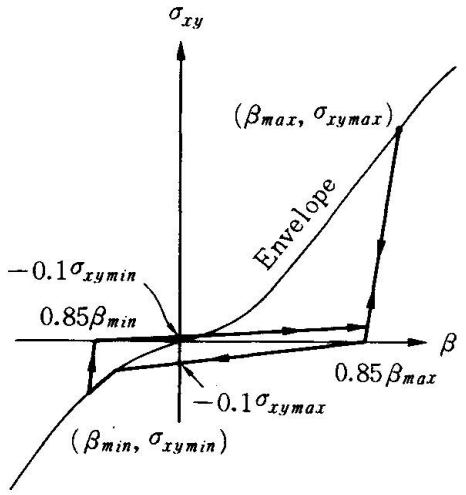

Fig.17 Shear transfer model for unloading and reloading

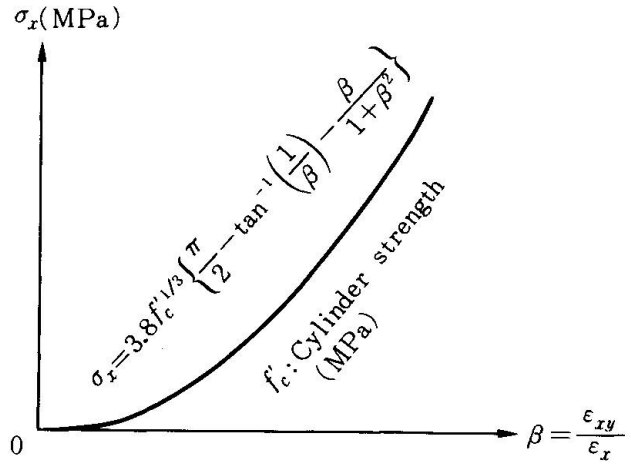

Fig.18 Compressive stress acting on the crack surface due to shear transfer

2.6 Steel Reinforcement Model in Concrete

As mentioned earlier, the tensile stiffness of a reinforced concrete may be represented by a superimposition of the tension stiffening due to concrete and the tensile stiffness the steel reinforcement develops. However, the constitutive laws for reinforcement need be modeled taking the bond to concrete into account, so that it should be different from that for an isolated steel reinforcement. Moreover, the stress acting on a reinforcement in between two cracks is not uniform because of the bond, taking on a maximum at the plane of crack as shown in Fig.19.

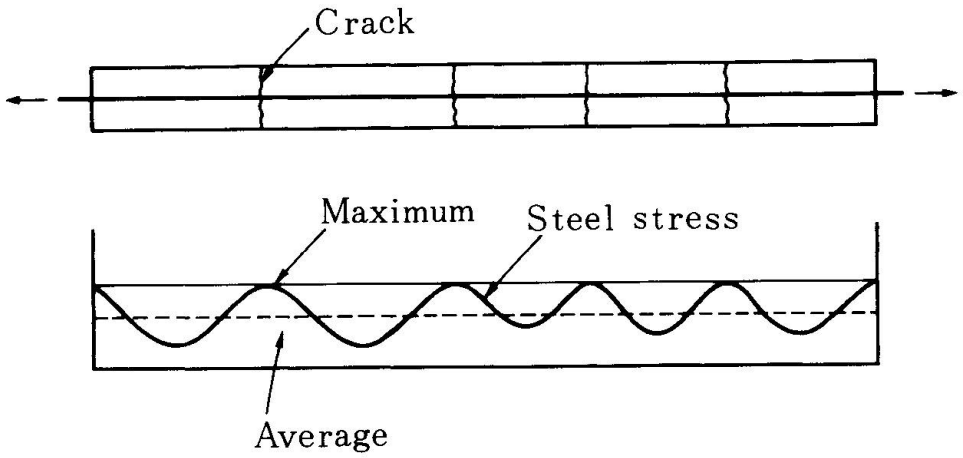

Fig.19 Stress distribution of reinfrocement in cracked concrete

As a reinforcement may be treated as elastic body until the stress acting on it reaches the yield strength of that reinforcement at the plane of concrete crack, the relation between the average stress and average strain is elastic as in the case of isolated reinforcement. Once the stress reaches the yield strength and the reinforcement yields, however, the stiffness that represents the average stress average strain relation suffers a rapid decrease. It is important to recognize that yielding of reinforced concrete as such takes place when the stress at the plane of concrete crack has reached the yield strength, not when the average stress in a reinforcement has become equal to the yield strength of isolated reinforcement. This difference is clearly shown in the uniaxial tensile testing of reinforced concrete element conducted by Tamai et al. as shown in Fig.20 [25]. It is also to be noted that the plastic strain shelf, which is often seen in the stress strain curve of isolated steel reinforcement, is not present in the cases of reinforced concrete, but the stress starts to increase monotonically with strain as in the strain hardening stage of isolated reinforcement.

One way of determining the average stress average strain relation after yielding of reinforcement is to assume a distribution profile for the reinforcement stresses acting in between cracks. Tamai et al. assumed this profile to be sinusoidal and the tensile stress of concrete remains in the same relation as that shown in Fig.5 even in the post yielding range. Calculations conducted for many panels, with the yield strength of reinforcement, strength of concrete, reinforcement ratio, difference in reinforcement ratio between two directions, and the angle between the cracks and reinforcement axes as parameters, showed that the average stress average strain relation may well be presented by a straight line shown in Fig.20.

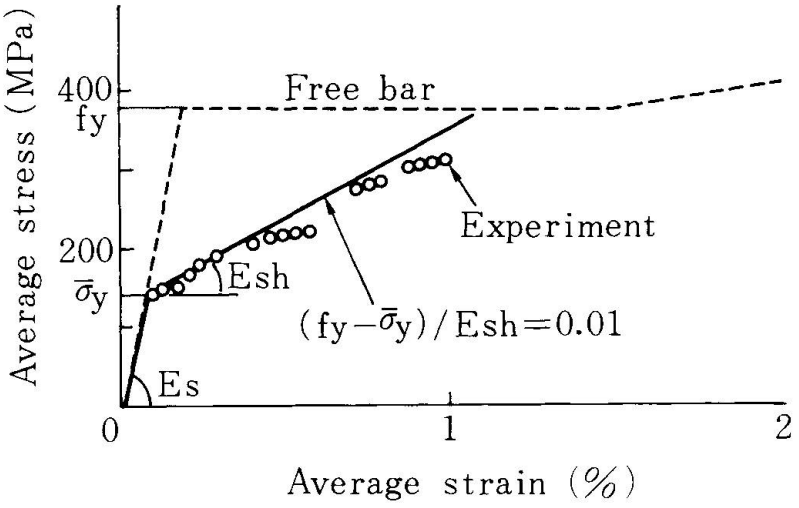

Fig.20 Average stress and average strain relation of reinforcement

As this apparent strain hardening rate is affected by the reinforcement bonding property, concrete strength, reinforcement ratio, reinforcement ratio difference between two directions, and angle between reinforcement and crack, a parameter has been provided to evaluate their effects integrally. As it was found, however, that these influences may be neglected without much aggravating the precision of calculation, the results presented herein are all those that were obtained with the parameter set equal to unity.

As for the constitutive rule for reinforcement in the unloading and reloading, the Kato's model [26] was adopted for its good agreement with the experimental results. To incorporate the Kato model in the method of Tamai et al. for determining the average stress average strain relation, reinforcement stresses corresponding to strains at various places along the bar axis should be integrated over the whole length to give an average. Since comparison of this method with the one involving the average strain of reinforcements as the reinforcement strain and the average stress of reinforcements as the reinforcement stress showed a very small difference when applied to the Kato model as shown in Fig.21, the more convenient latter mehtod has been used in the present study [22].

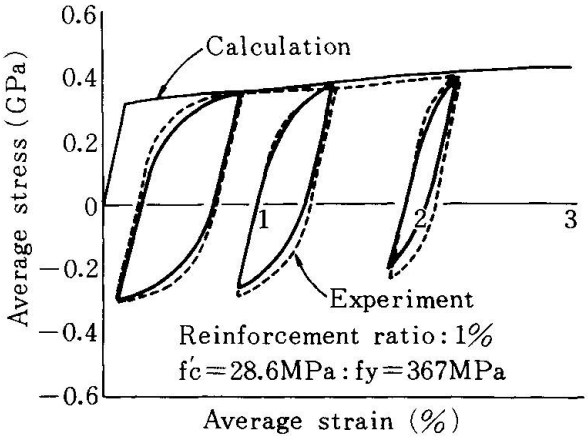

Fig.21 Steel reinfrocement in concrete under reversed cyclic loading compared with the experimental results [22]

3. ALGORITHM

The algorithm that computes out the stress strain relations for an element is shown as follows. It comprises a routine that calculates a strain increment for a given stress increment through a stiffness matrix to obtain the total strain and the stress that corresponds to it. This process is reiterated until the difference between the stress thus obtained and that given at first has become smaller than an appropriately given limit value.

The stiffness matrix is given for the first round of routine with a value that had originally been for the previous stress level. On the second round, the stiffness matrix is changed to the new one, but no further alterations are done for succeeding rounds. This practice is to take into account the large change that occurs in the stiffness matrix upon cracking of concrete and yielding of reinforcement. The stiffness matrix has been constructed using stiffnesses that are equal to or slightly larger than the tangential stiffness. For example, a zero stiffness is used for the negative stiffness that the tension stiffening model of concrete gives.

The concrete before cracking is assumed to be an elastic body, and upon occurrence of a crack, the direction of that crack is fixed in terms of the coordinates defined in Fig.1. Then, the stress is calculated from the strain in the concrete according to the constitutive rule for cracked concrete developed in section 2. In the meantime, the stress acting on a reinforcement is calculated from its strain by taking the reinforcement axes as the coordinates, and by converting the coordinates, these two stresses are superimposed each other to calculate the stress for the reinforced concrete.

On occurrence of the second crack, similar calculations are conducted in considering this crack alone. Subsequent calculations for concrete stiffness and reinforcement stiffness are done only for that crack which influences the more, though both cracks are taken into account in calculating the concrete shear stiffness.

For the unloading and reloading, material models that are suited for this process are used, meaning that the unloading and reloading of the materials are assumed to be in harmony with those of the element. This assumption is perfectly admissible in the single element analysis of the present work, but it is not without problems when many elements that are smaller than the crack spacing are involved. By making the size of element appropriately for objects that admit of applying the smeared crack model, these problems can generally be forestalled.

4. EVALUATIONS

As the comprehensive material models thus formulated so as to apply to reinforced concrete plate elements as described in section 2 have been developed on the results of comparatively simple experiments, applicability of the models was examined by comparing the calculations according to section 3 with the results of experiments conducted for reinforced concrete panels.

4.1 Envelopes

The calculated envelopes were assessed against the 17 panels from Vecchio-Collins' experiments, excluding those that the investigators themselves judged improper, and the 5 panels from Aoyagi-Yamada experiments, excluding the biaxial tensile test results. As an example, Fig.22 presents a comparison to the four panels from the Collins' competition, expect that here tensile

strengths of concrete that were in good accord with the experimental values were used for calculation. The agreement is quite satisfactory.

Similarly good agreements have been obtained for other experimental results. For example, for the ultimate strength, the average of ratios between experiments and calculations is 0.90 with regard to Vecchio-Collins and 1.08 to Aoyagi-Yamada, while the cofficient of variation is 8.6 % and 4.8 %, respectively.

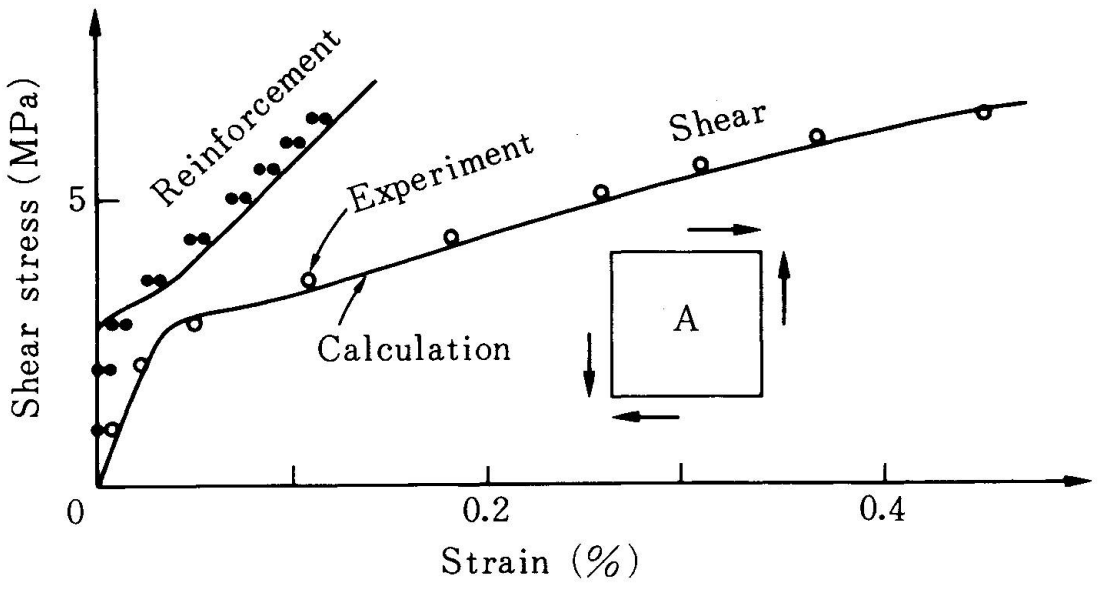

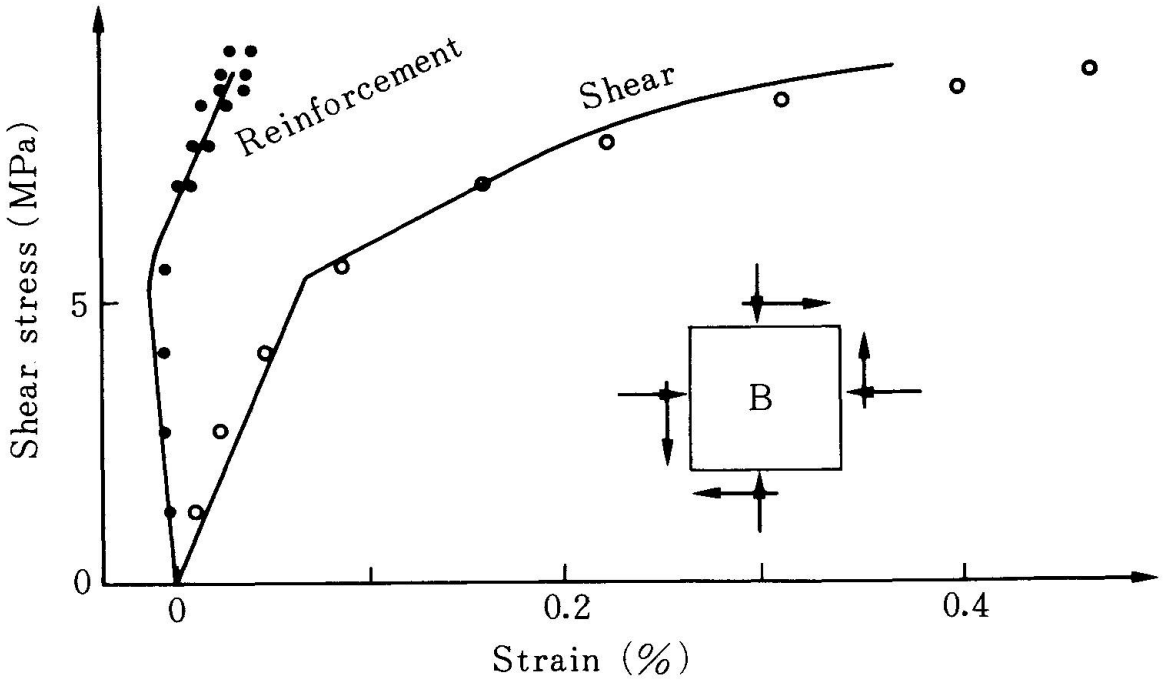

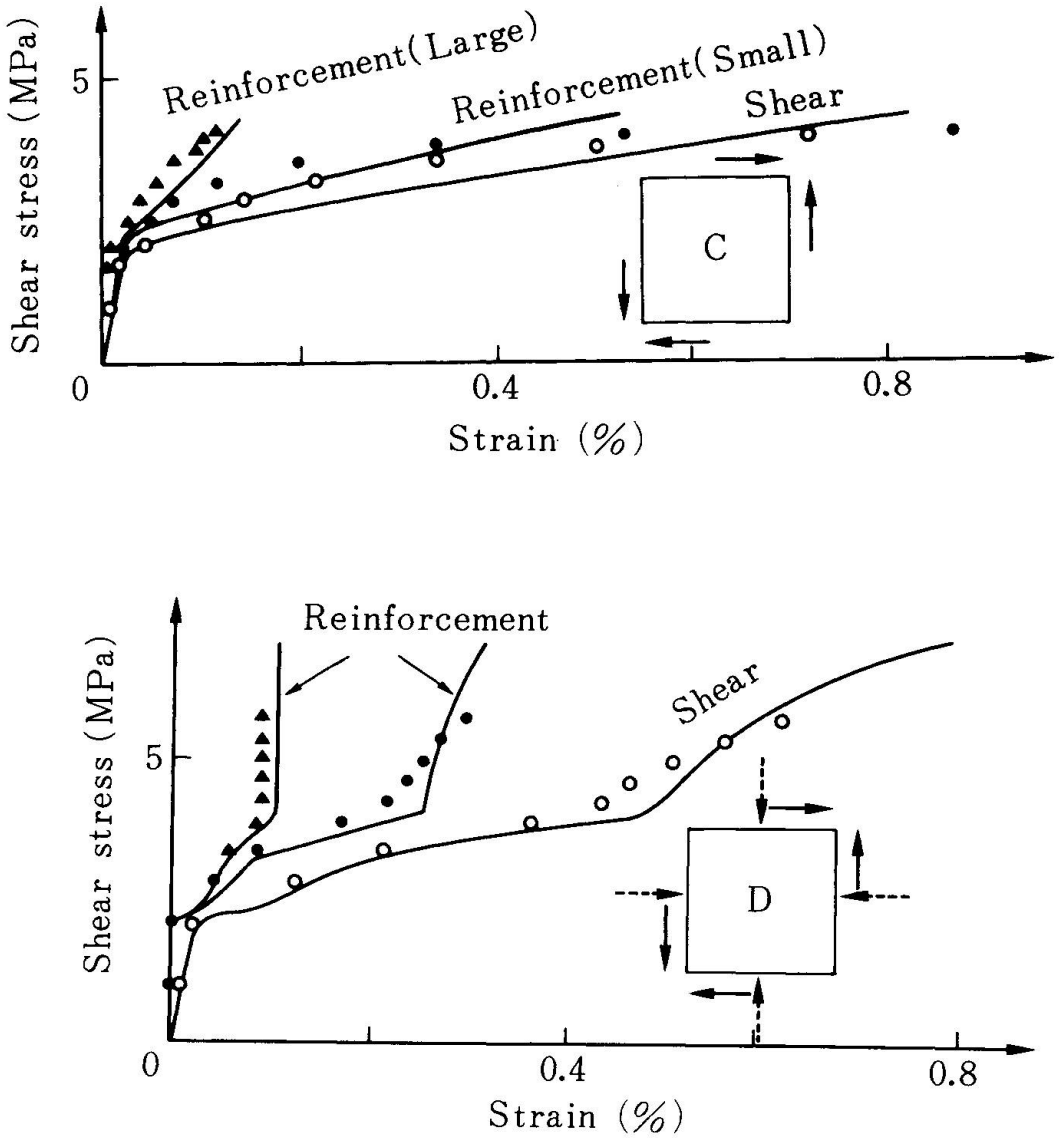

Fig.22 Comparison of the calculations with the experimental results by Vecchio - Collins for envelope

For the shear stress or tensile stress corresponding to a certain strain, 0.002 for example, the average ratios between experiments and calculations is 1.02 for Vecchio-Collins and 0.99 for Aoyagi-Yamada, where the cofficient of variation is 6.7% and 8.9%, respectively.

The ultimate strength for shear failure was assumed to be the stress corresponding to the shear strain along the crack plane of 0.004. The ultimate strength for compression failure was obtained when the compressive strain parallel to the crack plane exceeded that corresponding to the ultimate compressive strength of concrete. The ultimate strength for tension failure was defined as that when the average tensile strain of reinforcement reached the value of 0.01. Even though these values are admittedly in need of further examination, it was observed that small changes in those values gave rise to little changes in the ultimate strengths.

4.2 Cyclic Loading

The calculations for cyclic loading were evaluated against the results of Aoyagi-Yamada experiments [9]. The stress strain relations were faithfully reproduced even for the unloading and reloading as shown in Fig.23.

The results for reversed cyclic loading were compared to Yoshikawa's results [27] on torsion experiments of reinforced concrete cylinders, where no shearing stresses were acting in the plane of crack. As may be judged in Fig.24, the calculation is capable of tracing the element behaviors. However, roundness is somewhat lacking in the calculated behaviors, arising from the insufficient bulge that was given to the material models for unloading.

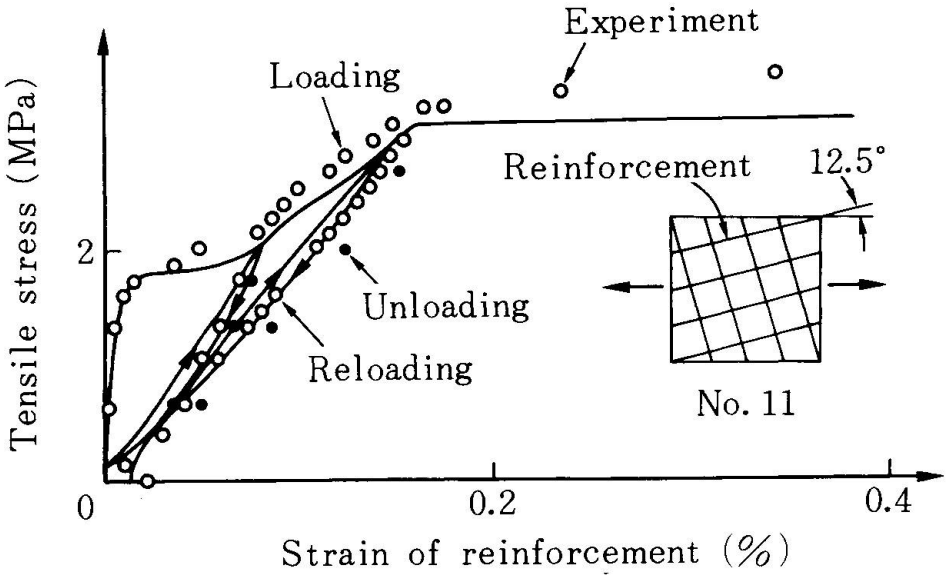

Fig.23 Comparison of the calculations with the experimental results by Aoyagi - Yamada for cyclic loading

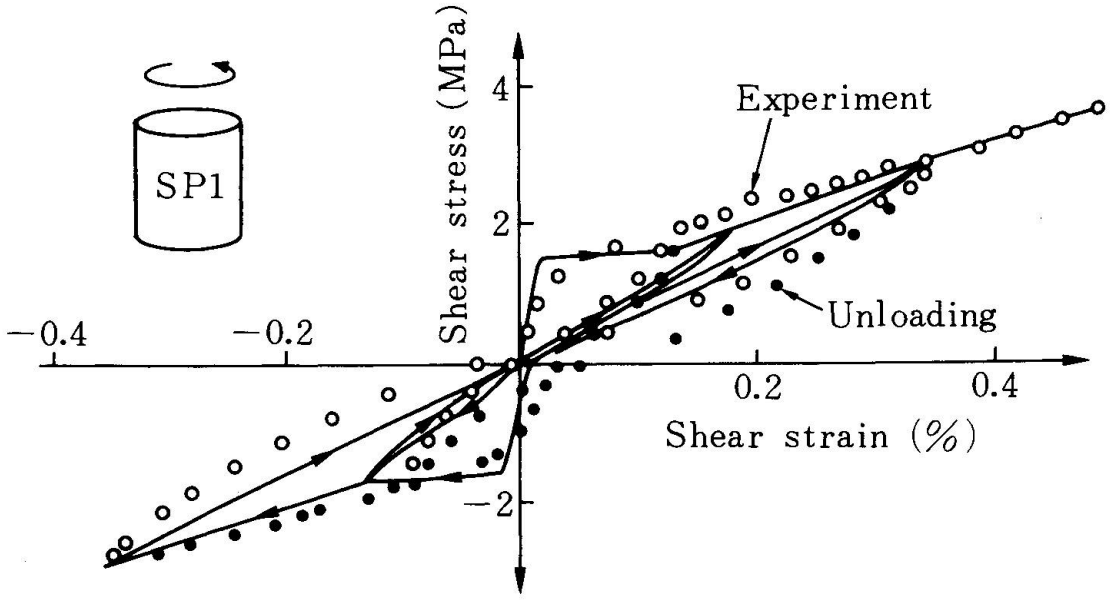

Fig.24 Comparison of the calculations with the experimental results by Yoshikawa et al. for reversed cyclic loading

5. Concluding Remarks

A comprehensive model for reinforced concrete plate element has been developed with comprising tension, compression, and shear models of cracked concrete and a model for reinforcement in the concrete. The applicability of this model has been verified by comparing with the results of experiments conducted for reinforced concrete panels.

The proposed reinforced concrete model can be applicable to predicting the envelope of a reinforced concrete panel subjected to in-plane forces fairly well. The proposed reinforced concrete model can be capable of tracing the plate element behaviors subjected to reversed cyclic loading. However, it would be necessary to use more accurate material models for unloading.

Acknowledgments

The authors would like to express their appreciation to our graduate students, Mr. Shin, H. Who helped to develop the analytical program for reinforced concrete plate elements, and Mr. Shima, H., Mr. Li, B., Mr. Tamai, S. and Mr. Miyahara, T., who successfully developed the material models for cracked concrete. The authors also are sincerely grateful to Dr. Yamada, K. and Dr. Yoshikawa, H. who willingly offered their valuable experimental data.

This research was supported by the Grant-in-Aid for Scientific Research No. 61420035 from the Japan Ministry of Education.

References

[1] Cervenka, V. and Gerstle, K.H., Inelastic Analysis of Reinforced Concrete Panels, Experimental Verification and Application, Publication, IABSE, Vol.32-II, 1972

[2] Darwin, D. and Pecknold, D.A., Analysis of RC Shear Panels under Cyclic Loading, Journal of ST Div., Proc. of ASCE, Vol. 102, No.ST2, Feb.1976

[3] Aktan, H.M. and Hanson, R.C., Nonlinear Cyclic Analysis of Reinforced Concrete Plane Stress Members, ACI Publication SP 63, 1980

[4] Sorensen, S.I., Plasticity and Endochronic Inelasticity in Finite Element Analysis of Reinforced Concrete, Final Report, Vol. Band 29, IABSE Colloquium, Copenhagen, 1979

[5] Noguchi, H., Analytical Models for Reinforced Concrete members Subjected to Reversed Cyclic Loading, Seminar on Finite Element Analysis of Reinforced Concrete Structure, JCI, Vol.2 Tokyo, May 20-24, 1985

[6] Collins,M.P., Vecchio,F. and Mehlorn,G., An International Competition to Predict the Response of Reinforced Concrete Panels, Festschrift Prof. Bruno Thurliman zum 60. Geburtstag, 1983

[7] Okamura,H., Maekawa, k. and Sivasubramaniyam,S., Verification of Modeling for Reinforced Concrete Finite Element, Finite Element Analysis of Reinforced Concrete Structure, Proc. of the Seminar ASCE, 1985

[8] Niwa,J., Maekawa,K. and Okamura,H., Nonlinear Finite Element Analysis of Deep Beams, Final Report IABSE Colloquium, Delft, 1981

[9] Aoyagi, Y. and Yamada,K., Strength and Deformation Characteristics of Reinforced Concrete Shell Elements Subjected to In-plane Forces, Proc. of JCSE, No.331, March, 1983, Concrete Library International No.4, 1984

[10] Maekawa,K. and Okamura,H., The Deformational Behavior and Constitutive Equation of Concrete using The Elasto-Plastic and Fracture Model, Journal of the Faculty of Engineering, The university of Tokyo Series B, Vol.37, No.2, Sept., 1983

[11] Muguruma,H. and Morita,S., Fundamental Study on Bond between Steel and

ADDENDUM

(insert before page 591)

Concrete (II.Defomation of Reinforced Concrete Tension Member),Trans.of AIJ, Sept., 1967 (in Japanese)
[12] Yoshikawa,H. and Tanabe,T., An Analytical Study for The Tension Stiffness of Reinforced Concrete Members on The Basis of Bond-Slip Mechanism, Proc. of JSCE ,No.366,Feb.,1986 (in Japanese)
[13] Somayaji,S. and Shah,S.P., Bond Stress versus Slip Relationship and Cracking Response of Tension Members, ACI Journal, Proc. Vol.78, No.3, May-June, 1981
[14] Leonhardt,F., Cracking Control in Concrete Structures, IABSE Survey S-4/77, Aug.1977
[15] CEB-FIP Model Code for Concrete Structures, 1987, pp.159
[16] Beeby,A.V., The Prediction of Crack Width in Hardened Concrete, Strucural Engineering (London), V57A, No.1, Jan., 1979
[17] Rizkalla,S.H. and Hwang,L.S., Crack Prediction for Members in Uniaxial Tension, ACI Journal, Proc. V81, Nov.-Dec., 1984
[18] Gilbert.R.I. and Warner,R.F., Tension Stiffening in Reinforced Concrete Slabs, Proc. of ASCE, V104, No.ST12, Dec., 1978
[19] Milford,R.V. and Schnobrich,W.C., Behavior of Reinforced Concrete Cooling Towers, University of Illinois at Urabana-Champaign, Illinois, May, 1984
[20] Morita,S. and Kaku,T., Experimental Study on the Deformation of Axially Reinforced Concrete Prisims subjected to Tension and Drying, CAJ Review of The 18th General Meeting, 1964
[21] Vecchio,F. and Collins,M.P., The Modified Compression Field Theory for Reinforced Concrete Elements Subjected to Shear, ACI Journal, March-April, 1986
[22] Tamai,S. and Shima,H., Tension Stiffening Effect under Reversed Cyclic Loading (under submitting JCI)
[23] Miyahara,T. and Maekawa,K., Nonlinear Behavior of Ccacked Reinforced Concrete Plate Element Under Unixial Compression, Proc. of JSCE, No.378, Feb., 1987 (in Japanese)
[24] Cervenka, V., Constitutive Model for Cracked Reinforced Concrete, ACI Journal, Nov.-Dec., 1985
[25] Tamai,S., Shima,H., Izumo,J. and Okamura,H., Average Stress-Average Strain Relationship of Steel in Uniaxial Tension Member in Post-Yield Range, Proc. of JSCE No.378, Feb.,1987 (in Japanese)
[26] Kato,B., Mechanical Properties of Steel Under Load Cycles Idealizing Seismic Actions, Bulletin D'Information, No.131, CEB, IABSE-CEB Symposium, May, 1979
[27] Yoshikawa,H., et al., Study on Shear Behavior of Concrete Container Vessel, Hazama Corporation Annual Report, 1983 (in Japanese)

Numerical Analysis of Thick Reinforced Concrete Slabs under Impact Loading

Analyse numérique des dalles épaisses en béton armé soumises à des chocs

Numerische Analyse dicker Stahlbetonplatten unter Stossbelastung

Josef EIBL
Prof. Dr.-Ing.
Institut für Massivbau
u. Baustofftechnologie
Karlsruhe, FRG

Josef Eibl, born 1936, graduated in Civil Eng. at the University of Munich; doctor's degree at the University of Braunschweig in 1962; professor in Braunschweig and Dortmund; since 1982 professor and director of the Institute of Concrete Structures and Building Materials at the University of Karlsruhe. Research field: reinforced concrete, impact, silos, constitutive equations.

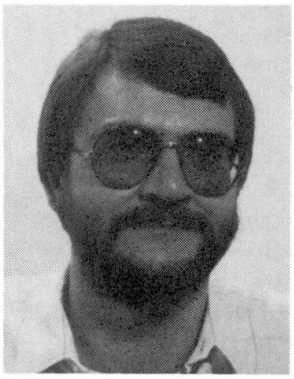

Franz-Hermann Schlüter, born 1956, graduated in Civil Engineering at the University of Dortmund. Since 1983 he is Research Fellow at the Institute of Concrete Structures and Building Materials at the University of Karlsruhe. Research field: computational analysis, constitutive equations, impact response of R.C. structures.

Franz-Hermann SCHLÜTER
Dipl.-Ing.
Institut für Massivbau
u. Baustofftechnologie
Karlsruhe, FRG

SUMMARY

The local response of impact loading on reinforced concrete structures is not yet clarified. The pure existence of FE-programs does not fulfill the demands of a design engineer. He has to know the constitutive input and he has to understand the influence of the different design parameters. Only this knowledge creates a reasonable design basis. Therefore, by means of an own developed FE-program which devotes special attention to the constitutive assumptions, parametric studies have been carried out to create such an understanding of the physical behaviour.

RÉSUMÉ

Le comportement local sous l'effet de chocs dans les structures en béton armé est mal connu. La simple existence de logiciels ne permet pas de répondre à toutes les questions de l'ingénieur projeteur. Celui-ci doit connaître les lois constitutives des matériaux et comprendre l'influence de différents paramètres du projet. Seule cette connaissance permet d'avoir une base raisonnable pour l'étude du projet. Un programme de calcul appliquant la méthode des éléments finis et tenant compte des lois constitutives des matériaux a été réalisé et comparé avec diverses études paramétriques pour créer une base solide du comportement physique.

ZUSAMMENFASSUNG

Über die lokalen Vorgänge bei Stoßbelastungen auf Stahlbetonbauteile besteht noch weitgehend Unklarheit. Auch wenn prinzipiell entsprechende EDV-Programme existieren, ist dem entwerfenden Ingenieur damit heute meist nur wenig gedient. Er wird sehr oft die stoffgesetzlichen Annahmen, wenn er sie überhaupt kennt, kritisieren müssen und er braucht ausgewertete Parameterstudien, die das komplexe Ineinandergreifen der verschiedensten Einflüsse klar erkennen lassen. Nur so erhält er eine Entscheidungsbasis für seine Entwürfe. Es wurde deshalb mit einem eigenen FE-Programm unter besonderer Berücksichtigung von stoffgesetzlichen Vorgaben sowie eigenen und fremden Versuchen Parameterstudien durchgeführt, um eine solide Ausgangsbasis zu schaffen.

1. THE PROBLEM

Impact loading is caused by the collision of at least two masses. For the civil engineer the special case where a moving mass - projectile - hits a structure is of dominant interest. The impact of a vehicle against a bridge column, a falling rock on a road shelter or an aircraft crash on the containment of a nuclear power plant represent such a situation.
Until now for the design of impact endangered reinforced concrete structures such as slabs and shells not many reliable procedures are available. Especially the common rules to treat local response, i.e. punching, are very sensitive with regard to the necessary amount of stirrups, and do neither include the influence of support conditions - contact of missile at the support or in the interior slab region -, nor the influence of bending reinforcement or the shape of the load-time-function.

Tests demonstrated clearly that there is a great influence of these mentioned parameters which is not fully understood. Slabs under nearly equal test configurations showed a quite different response, some being nearly undamaged, others being completely punched after a slight change of parameters (comp. [1],[2]). Although during the last years in a series of experimental and analytical investigations the impact problem has been treated (see e.g. [3],[4]), we still do not know which parameters influence the local behaviour in what way. For a safe and economic design however a detailed knowledge of material and structural behaviour is of considerable practical importance.

Therefore by means of an own developed FE-model which has been carefully checked and compared with experimental results to assure the validity of this analytical tool parameter studies on thick slabs have been performed. Thickness and span of the slabs, amount of bending and shear reinforcement, load distribution on the impacted area, shape of the load-time-function and support conditions were varied. The computational model and some typical results of this investigation will be presented .

2. COMPUTATIONAL MODEL

With regard to the available space just the main topics of the computational model will be presented . A detailed description is given in [5].

2.1 Finite Element Strategy

The nonlinear finite element analysis is carried out with an incremental solution strategy. After each time step equilibrium iterations are performed and the stiffness matrix is updated. Time integration is done by Newmark's scheme.

2.2 Discretisation

In practical cases it is sufficient to use an axisymmetric model for the examination of local responce because maximum local straining mostly occurs in the first impact phase. At this time there is still little influence of the boundary conditions. The slab does not 'know' whether it is rectangular or circular. However three-dimensional stress and strain states have to be considered.

The discretisation of the circular slab in a radial cross-section was done by 4-, 5- or 6-node isoparametric axisymmetric elements describing concrete as well

as reinforcement. Inertia effects are included using a lumped mass matrix. A typical FE-mesh used in the parameter study is shown in Fig. 3.
The external load is applied as uniform pressure load on a massless fictitious load-distribution-plate which is modeled with linear-elastic material (E = 210000 MPa) just above the impact zone. Contact elements, transfering only compressive stresses, connect this plate with the concrete structure. This plate is just a tool to avoid that load is applied to a node which in case of a material failure has no stiffness. In such a situation the load has to be distributed to other nodes. Furthermore the stiffness of the fictitious plate influences the stress distribution in the contact area, thus giving an impression of the consequences of different projectile rigidities.

2.3 Constitutive Assumptions

The three-dimensional constitutive model and failure criterion of OTTOSEN [6] served as a starting basis for the description of the material behaviour of a concrete element. Characteristics as dilatation under compressive stresses close to failure and softening behaviour in the postfailure region are included. As the original model is only designed for monotonic loading, the capability to describe un- and reloading with a Young's modulus parallel to the initial value was added (Fig. 1). To improve equilibrium iterations in the incremental solution algorithm the secant formulation of OTTOSEN was extended to a tangential formulation.
A smeared crack model was used to allow cracks to open and close. Special constitutive matrices for cracked elements have been developed. Tensile stresses perpendicular to a crack cannot occur, whereas shear stresses can be transmitted depending on the actuell crack width. The main effects of high strain rates are included additionally. This was done by a calibration of OTTOSEN's failure envelope with modified parameters at every time step.

For the reinforcement an elastic-plastic behaviour is assumed. A tension-stiffening effect, taking into account the concrete locally surrounding a rebar and stiffening it, was considered (Fig. 2).

3. PARAMETER STUDY

In a first step a reference slab, representing the lower bound of the nowadays used slabs in German nuclear power plants, was analysed with the following data:

Geometry (comp. Fig. 3)
- $d = 1{,}50$ m, $r = 10{,}80$ m, $a = 1{,}50$ m, $d_L = 0{,}10$ m

Concrete
- $E_b = 30000$ MPa, $\nu = 0{,}20$, $f_c = 35$ MPa, $f_t = 0{,}14 \cdot f_c$

Bending reinforcement
- BSt 1100/1300, $a_{s1} = 60$ cm²/m (bottom face), $a_{s2} = 50$ cm²/m (top face)

Stirrups
- BSt 420/500, $a_s = 66$ cm²/m².

Two different loading functions F(t) were considered (Fig. 4): first LF 1, the original function according to the German regulations for an airplane crash and second LF 2, a modification of that function with a steeper slope in the second ascend.
Using LF 1 the deformations develope as shown in Fig. 5. Due to the relative slow load ascend an overall bending deformation similar to a static loading can be observed. The highest tensile stresses occur first at the bottom face in near of the axis of symmetry forming nearly vertical orientated cracks (comp. Fig.6).

During the load history more and more cracks develope. The inclination of these cracks increases with the distance from the center of the slab. After nearly 40 ms a punching cone has formed which is connected essentially by stirrups with the remaining slab. At this time the stresses in the shear reinforcement are just below the ultimate stress of 500 MPa. They are plotted in Fig. 7. For comparison the dashed line indicates the assumed punching cone with an angle of $\alpha = 32,5°$ according to the German regulation KTA 2203. One can recognize that nearly no stressed stirrup crosses this line and that an angle $\alpha \simeq 45°$ would be much more realistic. The stress distribution of the bending reinforcement is shown in Fig. 8. Obviously the circumferential direction is more stressed than the radial one. After 100 ms nearly every circumferential rebar reaches its yield stress.

In a succeding calculation the thickness of the load-distribution-plate was increased from $d_L = 0,10$ m to $d_L = 0,50$ m in order to simulate a rigid projectile. This has the effect that now due to the local deformation of the concrete slab the load is not longer distributed uniformly over the impact area but is concentrated at the boundaries of the loaded area. The calculated stirrup-stresses are plotted in Fig. 9. Again the ultimate stesses of 500 MPa are nearly reached. Similar to the 'soft' load introduction a punching cone with $\alpha \simeq 45°$ can be observed. However in this case stirrups are activated just outside of the loadradius a (comp. Fig. 7). Under loading function LF 2 (Fig. 4) the slab is completly punched as well with 'soft' as with 'rigid' load introduction. Due to the steep second load ascend stirrups start cracking after ca. 38 ms. Only a cross-section of about $a_s = 100$ cm²/m² for the shear reinforcement could avoid a punching failure.

In a next analysis the thickness of the slab is increased to $d = 1,80$ m. With the above given reinforcement this slab resists both loading functions. However under LF 2 the stirrups reach their ultimate load bearing capacity.

A decreasing amount of bending reinforcement leads to another failure mechanism. As already shown in Fig. 5 the whole slab is showing an overall bending deformation, an effect which is emphasized by reduction of the flexural rigidity e.g. by less reinforcement. After the first ascend of the loading function the slab shows now big vertical bending cracks. If now the second ascend follows, the already damaged slab cannot resist this further straining. Punching failure occurs with a very steep angle.

As investigations of this type can only be done by large computer programs as the one mentioned for practical design purposes a simple design model on the basis of a two-mass-system has been developed giving in principally the same results. For details of this model the reader is refered to [5].

4. SUMMARY AND CONCLUSION

Many parameters influence the local behaviour of thick reinforced concrete slabs under impact. Often the response is quite sensitive to only a slight change of parameters. As result of the performed investigations it can be stated that thickness of the slab, span of the slab, support conditions, shear reinforcement, bending reinforcement, strength of concrete, shape of the loading function, magnitude of impacted area and load distribution on the impacted area all effect the punching behaviour significantly.

For design purpose a simple model consisting of a nonlinear two-mass-system is mentioned in [5].

REFERENCES

1. Jonas, W., Rüdiger, E. et al.: Kinetische Grenztragfähigkeit von Stahlbetonplatten. Bericht zum Forschungsvorhaben RS 165, Hochtief AG, Abt. Kerntechnischer Ingenieurbau, Frankfurt, 1982
2. Eibl, J., Kreuser, K.: Abschlußbericht zum Forschungsvorhaben 'Durchstanzfestigkeit von Stahlbetonplatten unter dynamischer Beanspruchung'. Lehrstuhl für Beton und Stahlbetonbau, Universität Dortmund, 1982
3. Plauk, G. (ed.): Proceedings of the RILEM-CEB-IABSE-Interassociation Symposium on Concrete Structures under Impact and Impulsive Loading. Berlin: Bundesanstalt für Materialprüfung, 1982
4. Eibl, J. (ed.): Berichte zum Forschungskolloquium 'Stoßartige Belastung von Stahlbetonbauteilen'. Abt. Bauwesen, Universität Dortmund, 1980
5. Schlüter, F.-H.: Das lokale Verhalten dicker Stahlbetonplatten unter stoßartiger Belastung. Dissertation Universität Karlsruhe, 1987 (in preparation)
6. CEB: Concrete under Multiaxial States of Stresses – Constitutive Equations for Practical Design. Bulletin d' Information No. 156, Paris, 1983

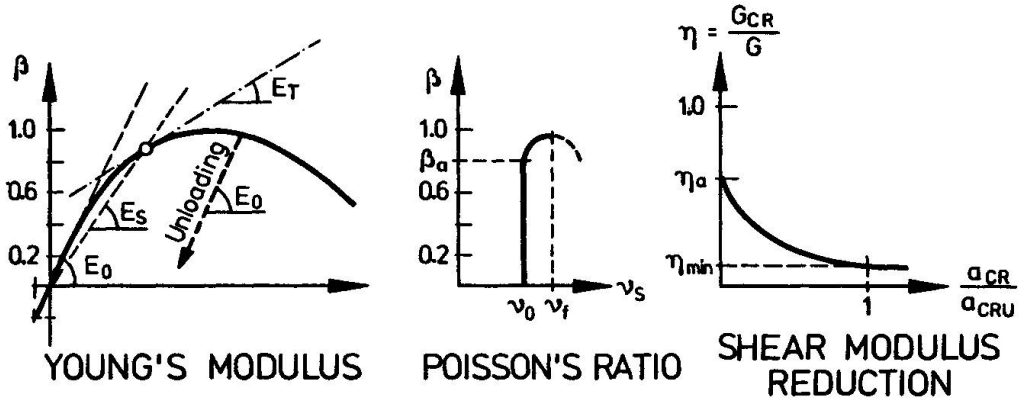

Figure 1: Modified triaxial constitutive assumptions for concrete resulting from [6]

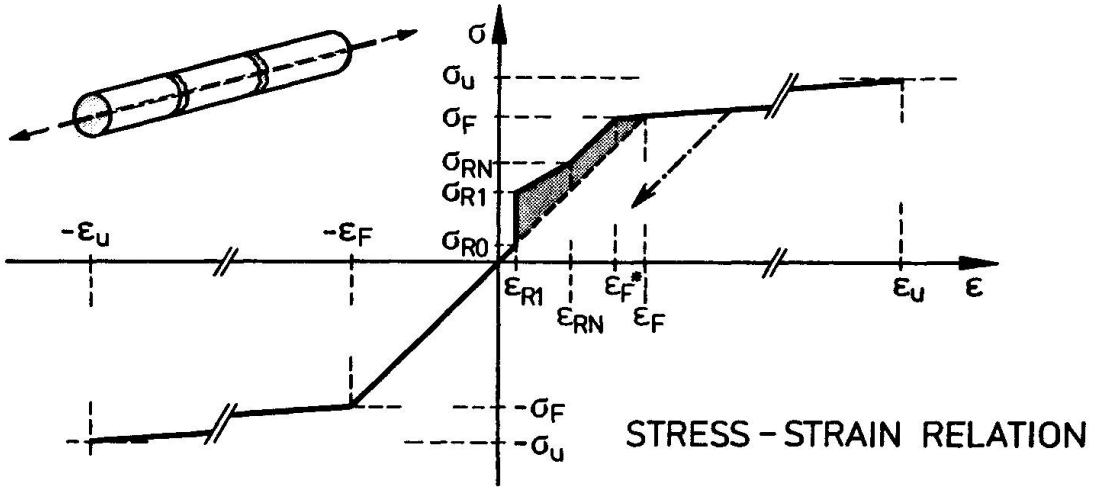

Figure 2: Constitutive assumptions for reinforcement including 'tension-stiffening'

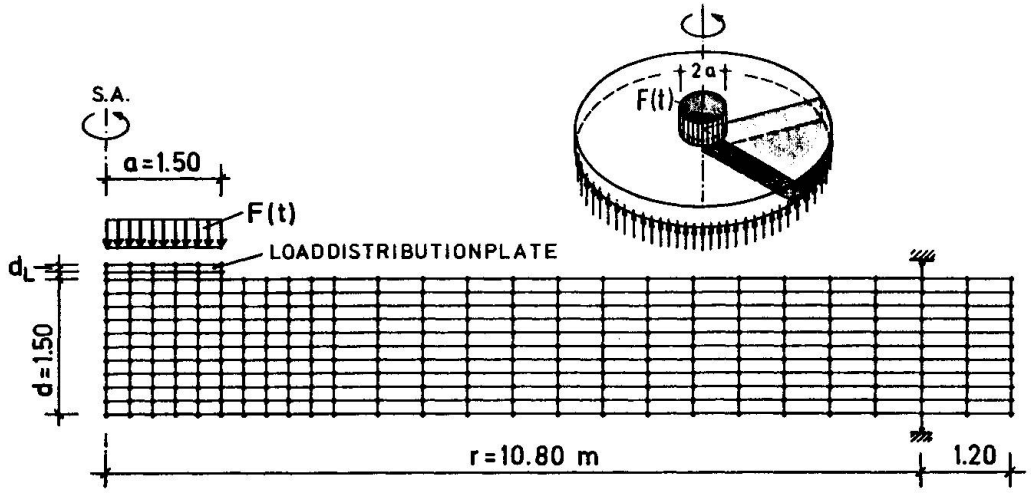

Figure 3: Discretisation of the axisymmetric slab

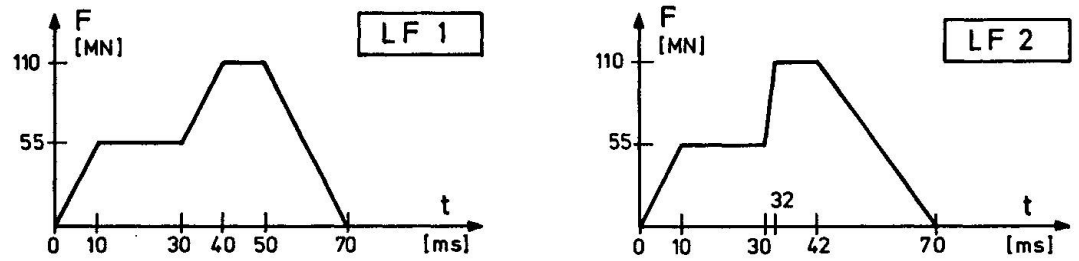

Figure 4: Applied load-time functions

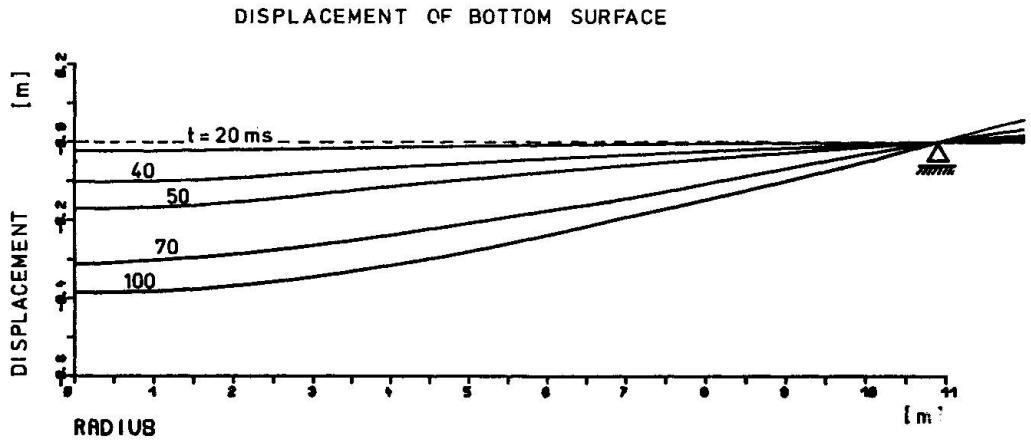

Figure 5: Deformation of the 1,50 m thick slab under LF 1 at different time steps

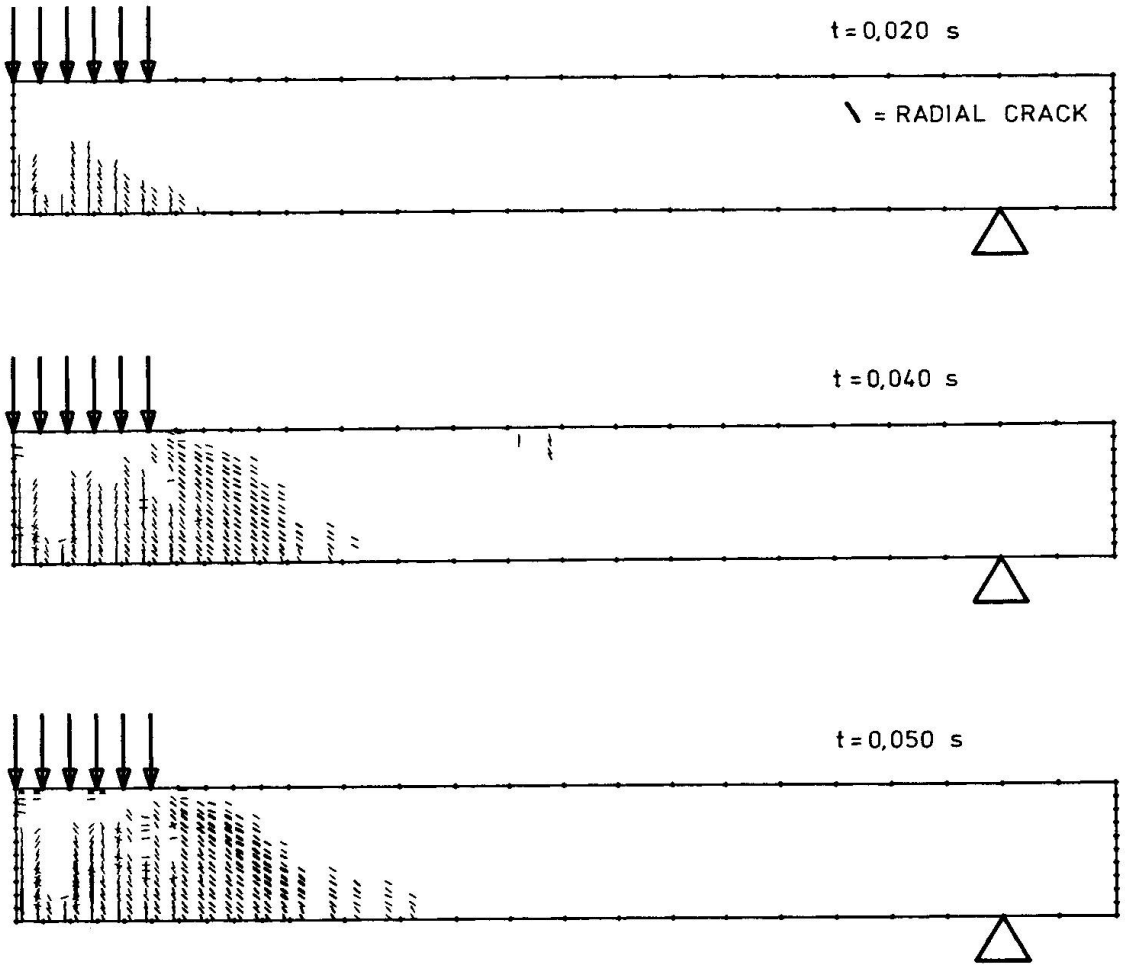

Figure 6: Developement of radial cracks of the 1,50 m thick slab

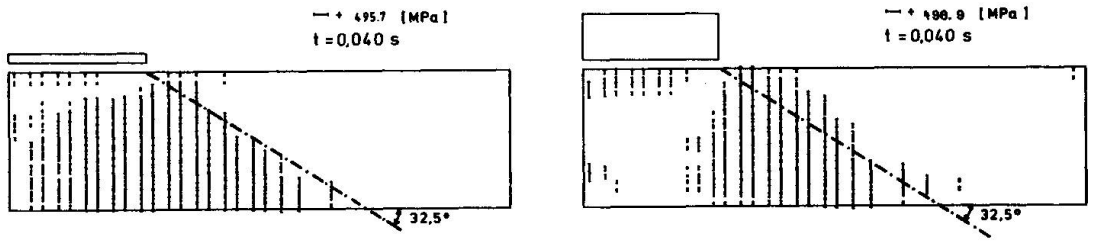

Figure 7: Stresses in stirrups at t = 40 ms a) with 'soft' and b) with 'rigid' load introduction

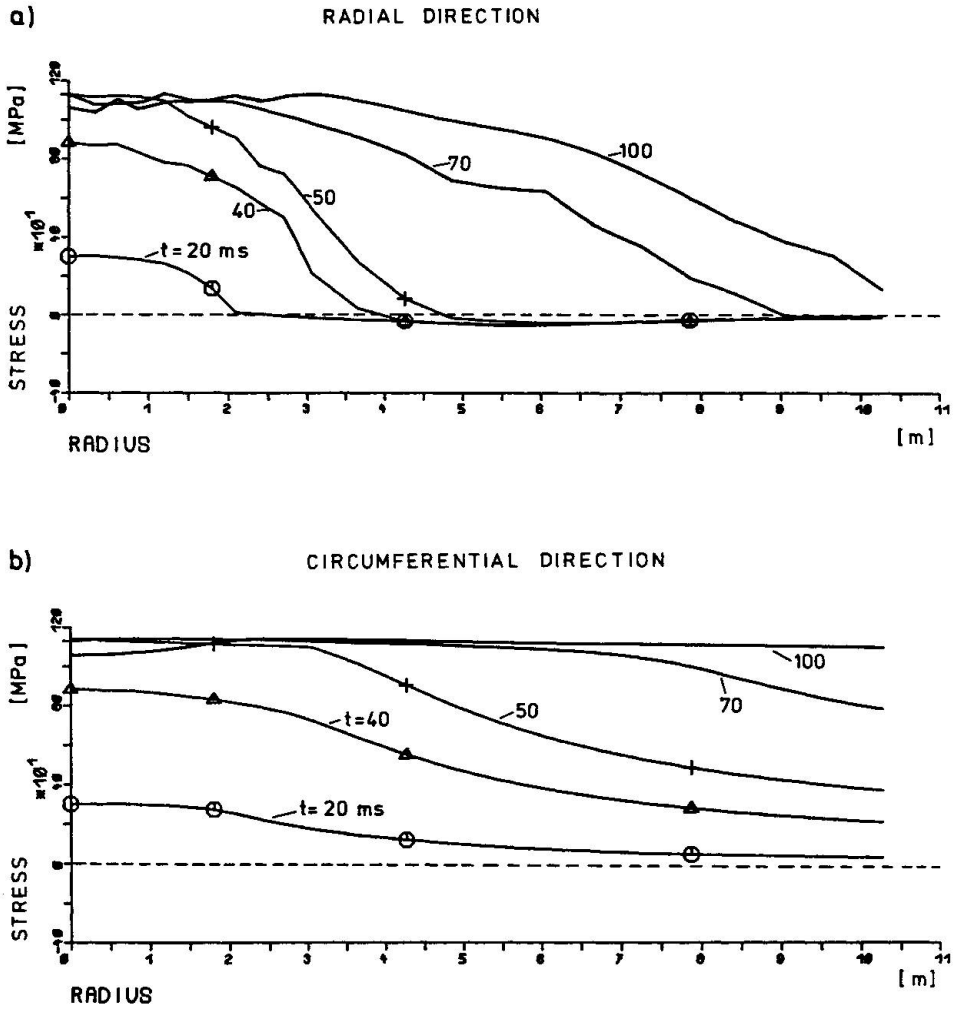

Figure 8: Stesses in bending reinforcement a) radial direction, b) circumferential direction

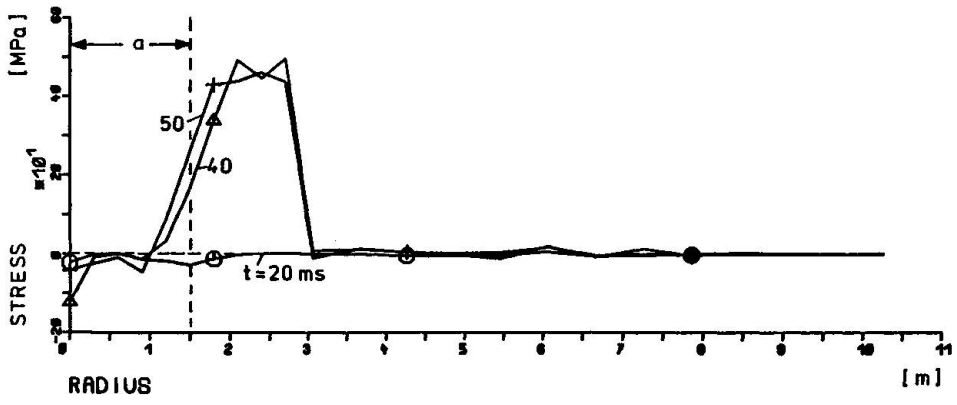

Figure 9: Stresses in stirrups with 'rigid' load introduction

Stress-Strain Based Inelastic Earthquake Response Analysis of Reinforced Concrete Frame Structures

Analyse de la réponse sismique inélastique des structures en béton armé

Unelastisches Erdbebenverhalten von Stahlbetonrahmentragwerken

Yoshikazu YAMADA
Professor
Kyoto University
Kyoto, Japan

Hirokazu IEMURA
Assoc. Professor
Kyoto University
Kyoto, Japan

Takashi MATSUMOTO
Senior Res. Engineer
Kajima Corporation
Tokyo, Japan

Danilo RISTIC
Assist. Professor
Univ. of 'Kiril and Metodij'
Skopje, Yugoslavia

Hachiro UKON
Research Engineer
Kajima Corporation
Tokyo, Japan

SUMMARY

This paper presents a method of stress-strain based inelastic earthquake response analysis of RC frame structures with varying axial forces. The material non-linearity of a RC element is evaluated by using a so-called 'fiber model' based on stress-strain relation. The accuracy of constitutive laws is examined by comparing of analytical and experimental moment-curvature relations. Earthquake response is calculated by step-by-step integration of the equation of motion. The method gives the most accurate estimation of inelastic earthquake response of RC structures.

RÉSUMÉ

Cet article présente une méthode d'analyse, basée sur le rapport entre la contrainte et la déformation, de la réponse sismique inélastique des structures en béton armé, analyse qui tient compte des forces axiales variables. La non-linéarité matérielle d'un élément en béton armé est évaluée avec un modèle appellé 'modèle fibre', reposant sur le rapport contrainte-déformation. La précision de ce rapport est estimée à partir de la comparaison des relations moment-courbure obtenues de façon analytique et expérimentale. La présente méthode assure la plus haute précision de l'évaluation de la réponse sismique inélastique des structures en béton armé.

ZUSAMMENFASSUNG

Im vorliegenden Beitrag wird eine Methode der auf der Spannungs-Dehnungs-Beziehung beruhenden nichtlinearen Erdbeben-Respons-Analyse von Stahlbetonrahmentragwerken bei variierenden Axialkräften gegeben. Die stoffliche Nichtlinearität eines Stahlbetonelements wird durch den Gebrauch eines sog. 'Faser-Modells' erfasst, das auf der Spannungs-Dehnungs-Beziehung basiert. Die Genauigkeit der konstitutiven Gesetze wird durch den Vergleich zwischen analystischen und experimentellen Momenten-Krümmungs-Beziehungen bestätigt. Die Methode liefert die genaueste Einschätzung des nichtlinearen Erdbeben-Respons der Stahlbetontragwerke.

I INTRODUCTION

With advance of construction technology and increase of transportation, large RC structures, such as cable-stayed PC girder bridges, arch bridges and high-rise buildings, have become feasible and practical, however, seismic safety of the structures are highly focused because of their social and economical importance.

Among them, seismic safety of RC frame towers of large cable-stayed bridges and RC columns of high-rise buildings is one of the most critical design problems in Japan. These structural members shall bear not only large bending moment but also high and time varying axial forces due to earthquake response of structures.

Recently, in designing RC structures the limit state design concept is becoming reasonable and popular in which the material non-linearity of an RC element needs to be considered. In the previous structural analysis of RC frame structures, material non-linearity were often assessed on the assumption of constant axial forces. In the case of statically indeterminate RC frame structures, however, the change of axial forces is an important factor to evaluate the safety of the whole structure. It is extremely complex and difficult to take account of variational axial forces in the conventional modeling[1] [2] of RC beam elements.

In this paper, a method of stress-strain based inelastic earthquake response analysis of RC frame structures with varying axial forces is proposed. Accuracy of the stress-strain models of concrete and steel is examined from the comparison of analytical and experimental moment-curvature relation of the cross section. A few numerical examples of earthquake response of RC structures are presented.

II NON-LINEAR ELEMENT STIFFNESS

1. Hysteretic rules of concrete and steel

Based on past experimental studies of stress-strain relations of structural materials under generalized cyclic loading, the stress-strain models for concrete and steel fibers are formulated including main parameters influencing these relations.

The Muguruma-Watanabe's rule[3] is modified to represent stress-strain relations of confined concrete fiber elements. In the model, concrete confinement levels[4], tension stresses, failure in tension, plastic strains, crush of concrete, compressive failure and stiffness degradation are described with nine different paths, five of which are previous path history dependent.

The Meneggoto-Pinto's rule[5] is adopted to represent stress-strain relation of steel fiber elements, which includes Baushinger effect, plastic strain and isotropic strain hardening for arbitrary strain history.

The adopted hysteretic rules of concrete and steel are schematically illustrated in Fig.1 and Fig.2. Details of the rules are presented in the reference[7].

2. Computation of non-linear element stiffness

Non-linear stiffness of a beam element is computed in the following algorism based on the beam theory.(See Fig.3) Three degrees of freedom(See Fig.4) are set at both end of a beam element.

1) To divide a beam element into some parts(Sub elements) along the axis line.
2) To compute axial strain ε_a and curvature strain ϕ at each dividing point from displacements at the ends of the element with the assumption that axial force is constant and bending moment varies linearly in the element.
3) To divide a section(Interface elements) at each dividing point into some parts (Fibers).
4) To compute strain ε_i at the location y_i of each Fiber using the assumption that a section remains flat.(Eq.(1))

$$\varepsilon_i = \varepsilon_a + \phi y_i \tag{1}$$

5) To obtain tangential stiffness E_i corresponds to ε_i at each Fiber using the aforementioned hysteretic rules.
6) To compute sectional stiffness $[K_{i.e.}]$ by integrating E_i over the Interface element.(Eq.(2))

$$\begin{Bmatrix} \Delta M \\ \Delta N \end{Bmatrix}_S = [K_{i.e.}] \begin{Bmatrix} \Delta\phi \\ \Delta\varepsilon_a \end{Bmatrix}_S \quad , \quad \text{where } [K_{i.e.}] = \begin{bmatrix} \sum A_i E_i y_i^2 & \sum A_i E_i y_i \\ \sum A_i E_i y_i & \sum A_i E_i \end{bmatrix} \tag{2}$$

7) To compute stiffness of Sub elements using the assumption of constant axial force and linearly varying bending moment in the element.
8) To compute stiffness of a beam element by integrating stiffness of Sub elements over the total length of the element.

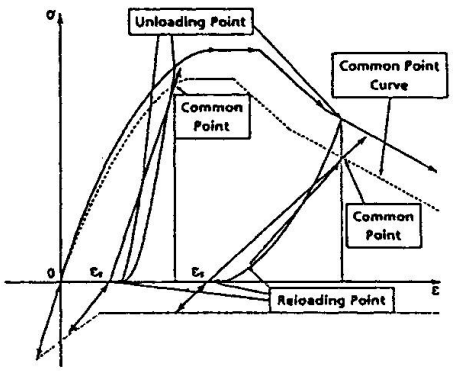

Fig.1 A hysteretic rule of concrete

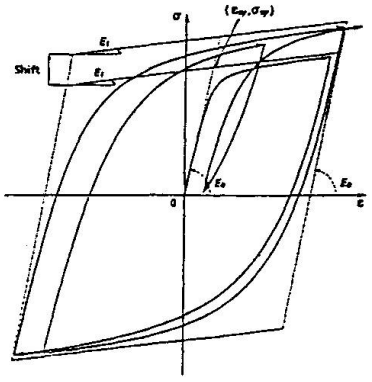

Fig.2 A hysteretic rule of steel

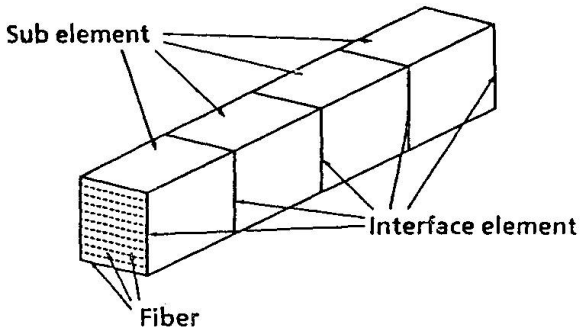

Fig.3 Division of a beam element

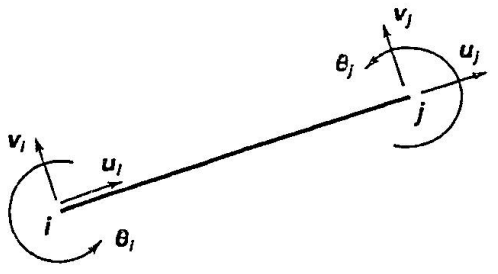

Fig.4 Degrees of freedom of a beam element

III COMPARISON OF EXPERIMENTAL AND ANALYTICAL MOMENT-CURVATURE RELATIONS

1. Results of hybrid loading tests

In order to obtain experimental results for the hysteretic behavior of RC elements under bending and time varying axial loads, a number of tests with the newly developed hybrid loading system of earthquake response(named as HYLSER shown in Fig.5) have been conducted, where earthquake response is calculated by a digital computer adopting the real hysteretic restoring force of elements which is directly measured from a loading actuator, of which details are found in the reference[6] [7] [8].

In the experiment, reinforced concrete specimens with cross section of 150×150 mm and total length of 2090 mm are used . The longitudinal reinforcement consists of 4×ϕ12.7mm steel bars. The lateral reinforcement of spiral tie hoops(ϕ=5mm) is adopted with pitches of 60mm and 90 mm. The cross section and its fiber model is shown in Fig.6. The hysteretic moment-curvature relations of the critical cross section of one of the tested specimens is plotted in Fig.7 for time intervals, t=0~10sec, t=10~20sec and t=20~30sec . In this case, N-S component of El-Centro record obtained during the Imperial Valley earthquake(5-18-1940) in the U. S. is used as an input earthquake ground motion. The time varying compressive axial force is controlled to be proportional to the restoring force of the specimen and plotted in Fig.8.

Generally, quite unique features of hysteretic loops due to time varying axial forces are found. In the moment positive side where axial force is increased, high but deteriorating restoring force is found due to spalling of concrete. On the contrary, in the moment negative side where axial force is decreased, low but non-deteriorating restoring force is found.

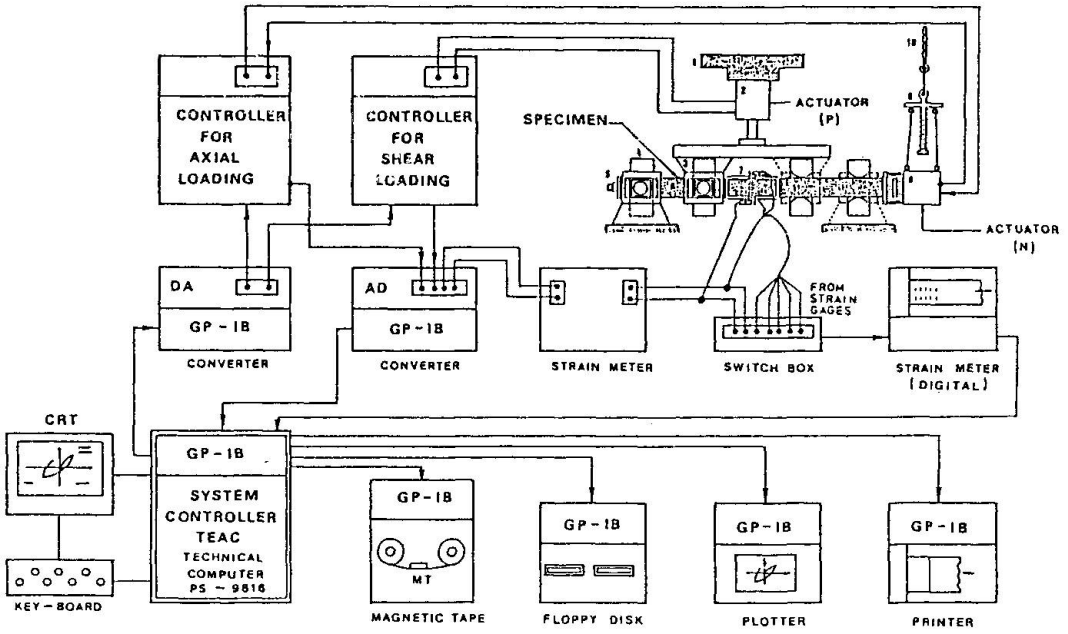

Fig.5 Diagram of the Online-Hybrid System

2. Analytical results from stress-strain model

Analytically calculated hysteretic moment-curvature relation is plotted in Fig.9 for the same time interval as shown in Fig.7. From the comparison of the experimental and analytical results, it is evident that complete pattern as well as corresponding moment and curvature levels are in good agreement even for this specific case where input curvature and axial force histories are given in quite irregular form. The empirically verified agreement encourages further coming stress-strain based dynamic analysis of RC frame structures.

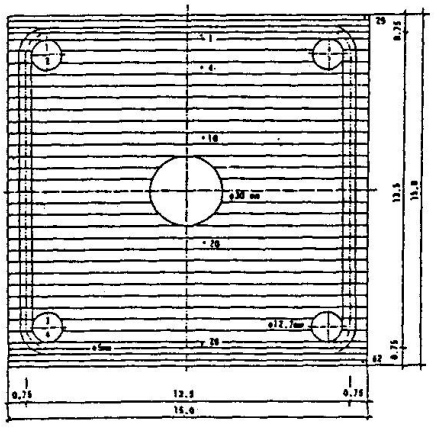

Fig.6 Cross Section Fiber Model

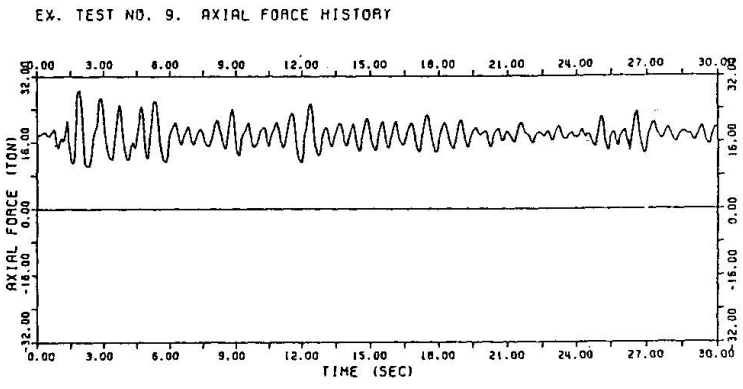

Fig.8 Time Varying Axial Force of the Specimen

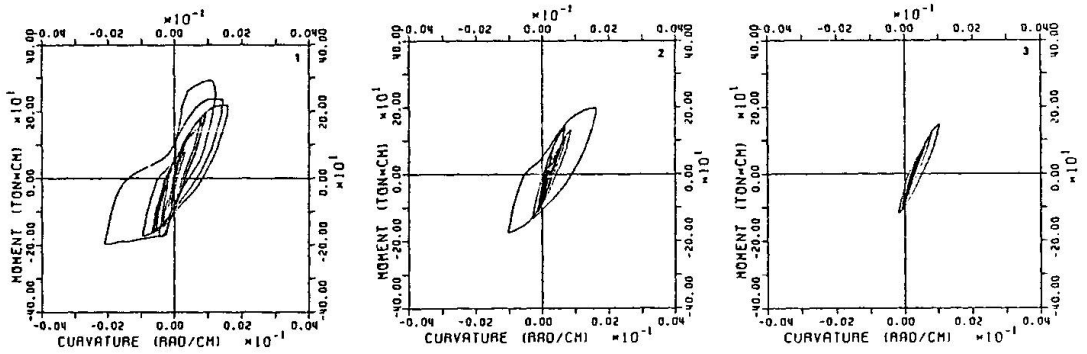

Fig.7 Experimental Moment-Curvature Relation of the Specimen in Every 10 Seconds of Earthquake Response

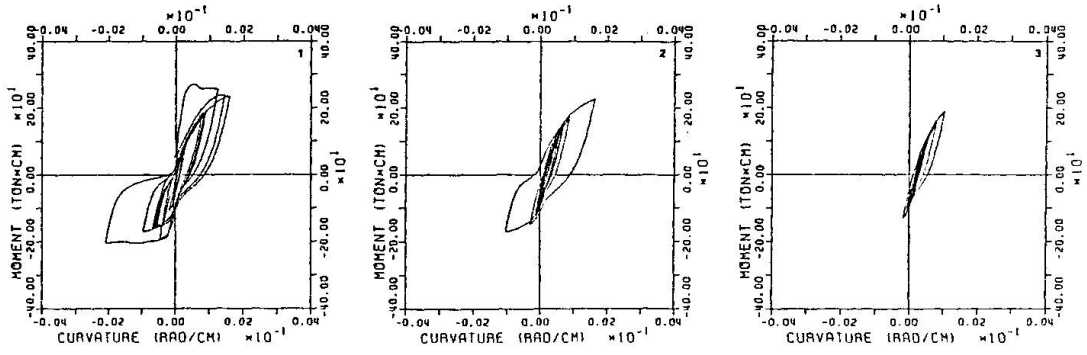

Fig.9 Analytically predicted Moment-Curvature Relation of the Specimen in Every 10 Seconds of Earthquake Response

IV DYNAMIC RESPONSE ANALYSIS

Since the afore-mentioned non-linear stiffness is time-variant, the basic equation of motion of a system is given in the following load incremental form using the assumption that stiffness is time-invariant in a short time step[9].

$$[M]\{\Delta\ddot{u}\} + [C]\{\Delta\dot{u}\} + [K]^t\{\Delta u\} = \{\Delta R\} \qquad (3)$$

where $[M]$: the mass matrix,
$[C]$: the damping matrix,
$[K]^t$: the stiffness matrix at time t,
$\{\Delta\ddot{u}\}$: the incremental acceleration vector,
$\{\Delta\dot{u}\}$: the incremental velocity vector,
$\{\Delta u\}$: the incremental displacement vector, $\{u,v,\theta\}$ for each node,
and $\{\Delta R\}$: the incremental earthquake force vector.

There are two main numerical problems to solve non-linear equations, that is, a problem of iteration and a problem of an unbalanced force. While a problem of numerical iteration should be mainly discussed on computing time and numerical accuracy, a problem of an unbalanced force should be also discussed including methodology how to compute it. The varying stiffness method is popular to consider an unbalanced force, though it generally requires a great amount of computing time. The equivalent external force method(or the initial stiffness method) is also becoming popular because it requires less computing time than the former method, however there is another problem that an impulse due to an equivalent external force is often generated in response.

The varying stiffness method with iteration is employed in this study because varying stiffness is computed at every time step according to the afore-mentioned algorism. However, from the practical view point, no iteration is performed in the following numerical examples.

In a computer program developed in this study, the consistent mass matrix and the lumped mass matrix can be employed alternatively as the mass matrix. Rayleigh damping matrix is used as the damping matrix. And Newmark's method and Wilson's θ method are available as a time integration scheme. The RC members can be alternatively processed as linear or non-linear elements.

V NUMERICAL EXAMPLES

1. A column model

To examine the effect of non-linearity, numerical examples of non-linear analysis(case-B) of a column model(10 elements, 11 nodes)(Fig.10) are compared with that of linear analysis(case-A). And the results in case-B are also compared with that of another non-linear analysis(case-C) in which the non-linearity of an RC element is assessed by M-ϕ hysteretic relation. The magnified El-Centro earthquake acceleration of which maximum value is 600(gal) is employed as an input ground motion. The time duration is 10.0(sec). The computing time increment is 0.005(sec). The structural and material constants used in this example are summarized in the following. The consistent mass matrix and Wilson's θ method are employed.

- Structural constants

$A = 1.0\text{m}^2$ $\quad h = 10.0\text{m}$

$A_s = 0.030\text{m}^2$

- Material constants

$\sigma_{ck} = 4000.0t/\text{m}^2$ $\quad \sigma_{cu} = 2000.0t/\text{m}^2$

$\sigma_{tk} = 100.0t/\text{m}^2$ $\quad \sigma_{sy} = 30000.0t/\text{m}^2$

$\varepsilon_{cy} = 0.0020$ $\quad \varepsilon_{cr} = 0.0024$

$\varepsilon_{cu} = 0.0100$ $\quad \varepsilon_{cl} = 0.0210$

$\varepsilon_{sy} = 0.0010$ $\quad \gamma_c = 2.0t/\text{m}^3$

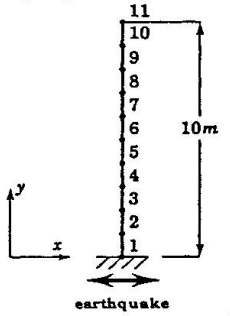

Fig.10 A column model

Fig.11 and Fig.12 show the acceleration response of the top-end point in case-A and in case-B respectively. Fig.13 shows the displacement response of the same point in case-B. Fig.14 shows the displacement response of the same point in case-C. Fig.11, Fig.12 and Fig.13 show that the frequency of acceleration response in case-B becomes lower than in case-A, the maximum value of acceleration in case-B is smaller than in case-A(86.6%) and the maximum value of displacement in case-B is bigger than in case-A(134.5%). These results are explained by the effect of material non-linearity, that is, the degradation of the system. Fig.14(case-C) shows a good agreement with Fig.13(case-B). Hence, M-ϕ model(case-C) may be satisfactory when there is no change in axial force.

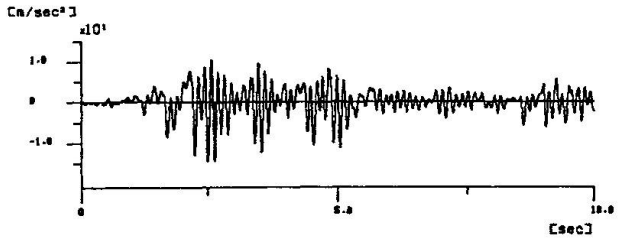

Fig.11 Acceleration response in case-A

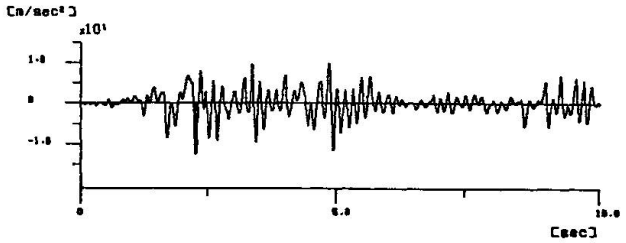

Fig.12 Acceleration response in case-B

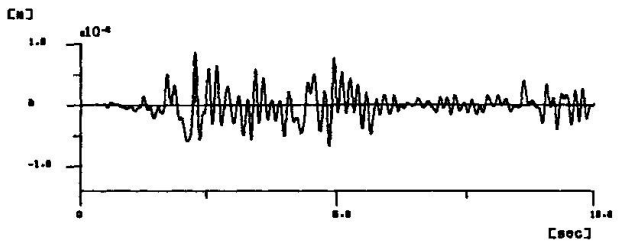

Fig.13 Displacement response in case-B

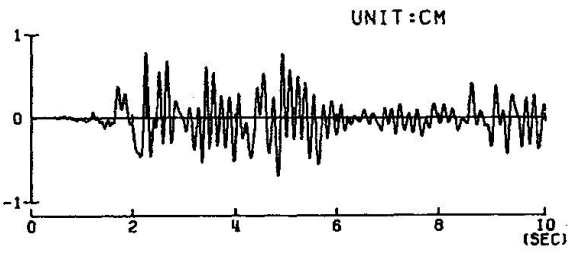

Fig.14 Displacement response in case-C

2. An RC tower model of a cable-stayed PC girder bridge

Numerical examples of an RC tower model(24 elements, 25nodes)(Fig.15) of a cable-stayed PC girder bridge of which span length is more than 200 meters are computed. The input earthquake motion is the same as in the first numerical example. The duration time is 6.0 (sec). The computing time increment is 0.005(sec). The material constants and others used in this example are summarized in the following.

- Material constants

$\sigma_{ck} = 3400.0t/m^2$ $\quad \sigma_{cu} = 1700.0t/m^2$
$\sigma_{tk} = 340.0t/m^2$ $\quad \sigma_{sy} = 30000.0t/m^2$
$\varepsilon_{cy} = 0.0020$ $\quad \varepsilon_{cr} = 0.0024$
$\varepsilon_{cu} = 0.0100$ $\quad \varepsilon_{cl} = 0.0210$
$\varepsilon_{sy} = 0.0015$ $\quad \gamma_c = 2.35t/m^3$

- Damping constants

$\alpha = 0.0$ $\quad \beta = 0.0318$

- Integration scheme(Newmark's method)

$\delta = 1/2$ $\quad \alpha = 1/4$

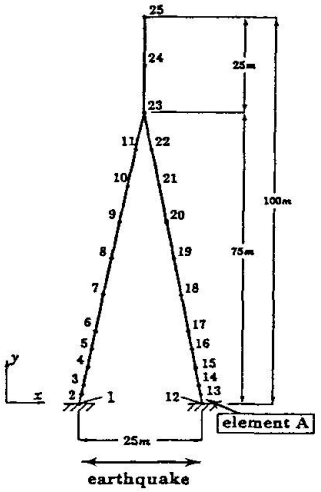

Fig.15 An RC tower model

Fig.16 and Fig.17 show the acceleration and the displacement response at the top respectively. Fig.18 and Fig.19 show the axial force(N) and the bending moment(M) response of the right-side bottom-end element(element A in Fig.15) respectively. The stress-strain relation of concrete, that of steel and M-N relation of the element are shown in Fig.20, Fig.21 and Fig.22 respectively. M-ϕ relation of the element is shown in Fig.23. Fig.24 and Fig.25 show the non-stational spectra of the response in Fig.16 and that of acceleration response by linear analysis. These results show the inelastic behavior that acceleration becomes smaller(85.3%), displacement becomes bigger(320.5%) and bending moment becomes smaller(71.7%) than the results by linear analysis. As to axial force, the change of it must have a great effect on the seismic safety of the structure because the varying range of N may be up to 15000.0(ton) in the example(Fig.18) and there is a basic linear relation between N and M(Fig.22). Besides, M-ϕ relation is much affected by the varying axial force(Fig.23). On the other hand, the initial sectional force due to own weight, cable tension or the initial maladjustment of structure is another important factor to the seismic safety of structure because it determines the starting point of stress-strain relation(Fig.20, Fig.21). Among them, the initial sectional force due to the initial maladjustment has a serious effect on the change of N because it is uncertain in nature and causes big initial sectional forces. Fig.24 shows the process of the degradation of the system by the non-linear analysis while Fig.25 shows no degradation, that is, the dominant frequency of the response remains unchanged.

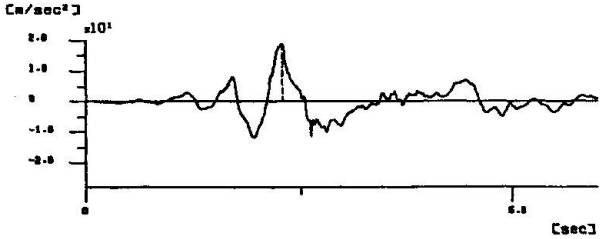

Fig.16 Acceleration response at the top

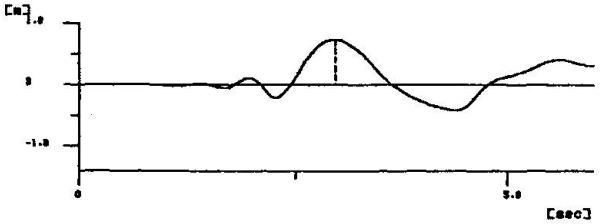

Fig.17 Displacement response at the top

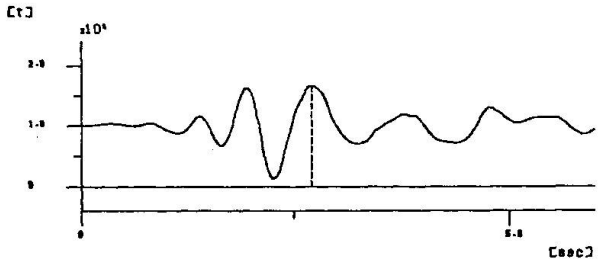

Fig.18 Axial force response at A

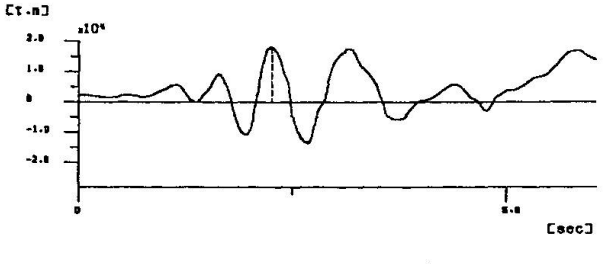

Fig.19 Bending moment response at A

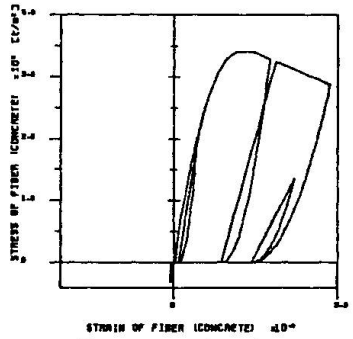

Fig.20 Stress-strain of concrete

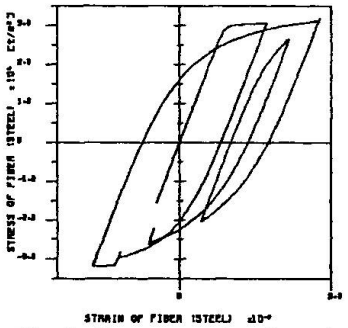

Fig.21 Stress-strain of steel

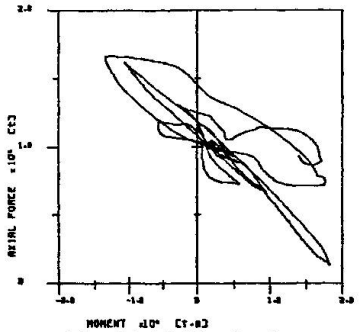

Fig.22 *M-N* relation

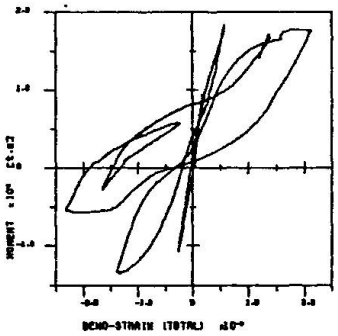

Fig.23 *M-φ* relation

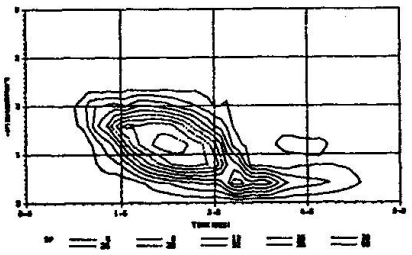

Fig.24 Spectrum of Fig.16

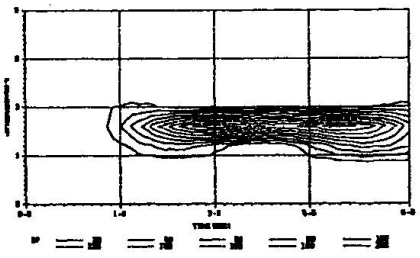

Fig.25 Spectrum of linear response

VI CONCLUSIONS

In this study, a method of stress-strain based inelastic earthquake response analysis of RC frame structures with varying axial forces is presented, and following conclusions are obtained.

(1) Moment-curvature relations analytically estimated from stress-strain relations used in this study agree fairly well with the experimental results of earthquake response.
(2) A varying axial force has a nonnegligible effect on *M-φ* relation of a section and the seismic response of an RC frame structures.
(3) The strength in the axial force increasing side and the ductility in the axial force decreasing side shall be checked for earthquake resistant design of the structures
(4) The varying range of axial force may become more than the degree of the initial axial force, depending on configuration of an RC frame structures.
(5) The initial sectional force due to the initial maladjustment has a great effect on the seismic response of an RC frame structure.

REFERENCES

1. Otani,S., ; "SAKE-A Computer Program for Inelastic Response of R/C Frames to Earthquakes", Civil Engineering Studies, Structural Research Series No.413, University of Illinois, Urbana, November, 1974.

2. Bertero,V. V. and Povov,E. P., ; "Hysteretic Behavior of Ductile Moment-Resisting Reinforced Concrete Frames Components", EERC Report No. &%/16, University of California, Barkeley, April, 1975.

3. Muguruma,H., Watanabe,F., Iwashimizu,T. and Mitsueda,R., ; "Ductility Improvement of High Strength Concrete by Lateral Confinement", Transactions of Japan Concrete Institute, Vol. 5, 1983, pp. 403-410.

4. Park,R., Priestly,N. and Gill,W.D., ; "Ductility of Square Confined Concrete Columns", Journal of Structural Division, ASCE, Vol. 108, No. ST4, April, 1982, pp. 929-950.

5. Menengotto,M. and Pinto,P., ; "Method of Analysis for Cyclically Loaded Reinforced Concrete Plane Frames Including Changes in Geometry and Nonelastic Behavior of Elements under Combined Normal Force and Bending", IABSE Symposium on Resistance and Ultimate Deformability of Structures Acted on by Well-Defined Repeated Loads, Final Report, Lisbon, 1973.

6. Iemura,H., ; "Hybrid Experiments on Earthquake Failure Criteria of Reinforced Concrete Structures", Proceedings of the 8th WCEE, San Francisco, Vol. VI, pp. 103-110, 1984

7. Ristić,D., Yamada,Y. and Iemura,H., ; "Stress-Strain Based Modeling of Hysteretic Structures Under Earthquake Induced Bending and Varying Axial Loads - Development and Verification - ", Research report NO.86-ST-01 , School of Civil Engineering, Kyoto University , 1986.

8. Iemura,H., Geshi,Y. and Maeda,S., ; "Hybrid Experiments on Inelastic Flexural Earthquake Response of RC Members with Varying Axial Forces", Proc. of the 7th Japan Earthquake Engineering Symposium, pp. 1207-1212, 1986.

9. Bathe,K.-J. and Wilson,E.L. ; "NONSAP-A General Finite Element Program for Nonlinear Dynamic Analysis of Complex Structures", Paper M3-1, Proceedings, 2nd Int. Conf. on Structural Mechanics in Reactor Tech., Berlin, Germany, Sept. 1973.